THE ASTRONOMICAL JOURNAL

PUBLISHED BY THE AMERICAN INSTITUTE OF PHYSICS
FOR THE AMERICAN ASTRONOMICAL SOCIETY

VOLUME 66 August 1961 ~ No. 1291 *NUMBER 6*

The Fornax Dwarf Galaxy. II. The Distribution of Stars

Paul W. Hodge*
Mount Wilson and Palomar Observatories, Carnegie Institution of Washington, California Institute of Technology

(Received April 27, 1961)

From counts of 60 000 stars in the neighborhood of the Fornax dwarf galaxy, the distribution of the projected stellar density in the galaxy has been derived. It is found to be smooth, with its ellipticity averaging about 0.35, and with some asymmetry in the central region. The density profile falls off more rapidly with distance than Hubble's interpolation formula for giant ellipticals. This is interpreted as the result of the gravitational influence of the Galaxy on the outer stars of the Fornax dwarf. From estimates of the mass of Fornax it is found that the predicted tidal limiting radius is in reasonable agreement with that observed. There does not appear to be any general obscuration within the galaxy; distant galaxies are distributed uniformly behind it.

I. INTRODUCTION

THE distribution of luminosity with radius for elliptical galaxies has been the subject of numerous studies (Hubble 1930; Redman and Shirley 1938; de Vaucouleurs 1948; Baum 1956; Liller 1960; and many others). In general, these investigators have ound that the interpolation formula employed by Hubble fits the intensity distribution of giant elliptical galaxies well, although there seems to be a tendency for he luminosity to fall off more rapidly than the law at great distances. Almost without exception the elliptical galaxies so far examined photometrically, of which there are some 50, have been giant objects of high luminosity with bright nuclei and steep luminosity gradients. Two exceptions are NGC 205 and M32, which have been measured by Redman and Shirley (1938), Sytinskaya (1943), and van Houten, Oort, and Hiltner (1954). Both of these galaxies have moderate absolute magnitudes, bright nuclei, and fairly steep luminosity gradients. There are no published measures, however, of the kind of elliptical that appears to be the most abundant type, that is, the Sculptor-type dwarf ellipticals, which have faint absolute magnitudes, no nuclei, and very low luminosity gradients.

This paper reports the examination of the structure of one such galaxy, the Fornax dwarf [$\alpha=2^h38^m$, $\delta=-34°.7$ (1950)], discovered by Shapley (1938) (Fig. 1). It is apparently the largest and most populous of the Sculptor-type galaxies in the local group, and the only one to contain globular clusters (Baade and Hubble 1939; Shapley 1939; Hodge 1961). Its distance is approximately 188 kpc, as determined by Baade and Hubble (1939), who measured the brightest stars in two of the globular clusters by photographic transfers. (There are three sources of error in this determination: the errors in the primary sequence used, the errors due to the photographic transfer from a sequence to the very low altitude reached by Fornax at Mount Wilson, and the uncertainty in the identification of the magnitude of the brightest stars in Fornax's globular clusters with any particular absolute magnitudes. These total at least 0.5 magnitude and probably more.)

The Fornax dwarf galaxy has such an extremely low surface brightness that conventional methods of determining the distribution of intensity are relatively ineffective. Photoelectric scans across the face of the Fornax dwarf have not yet been successful. Small-camera photographs can be obtained which show the galaxy, but only the central portion. Large reflectors can detect the individual brightest stars, but the small field limits them to only a fraction of the galaxy on any one plate. Therefore, the most effective method of determining the structure of such an object with present equipment is by means of star counts on Schmidt plates, which have large enough fields to show the whole galaxy and a large area around it, and which are capable of very faint limiting magnitudes.

---

* National Science Foundation Post-doctoral Fellow.

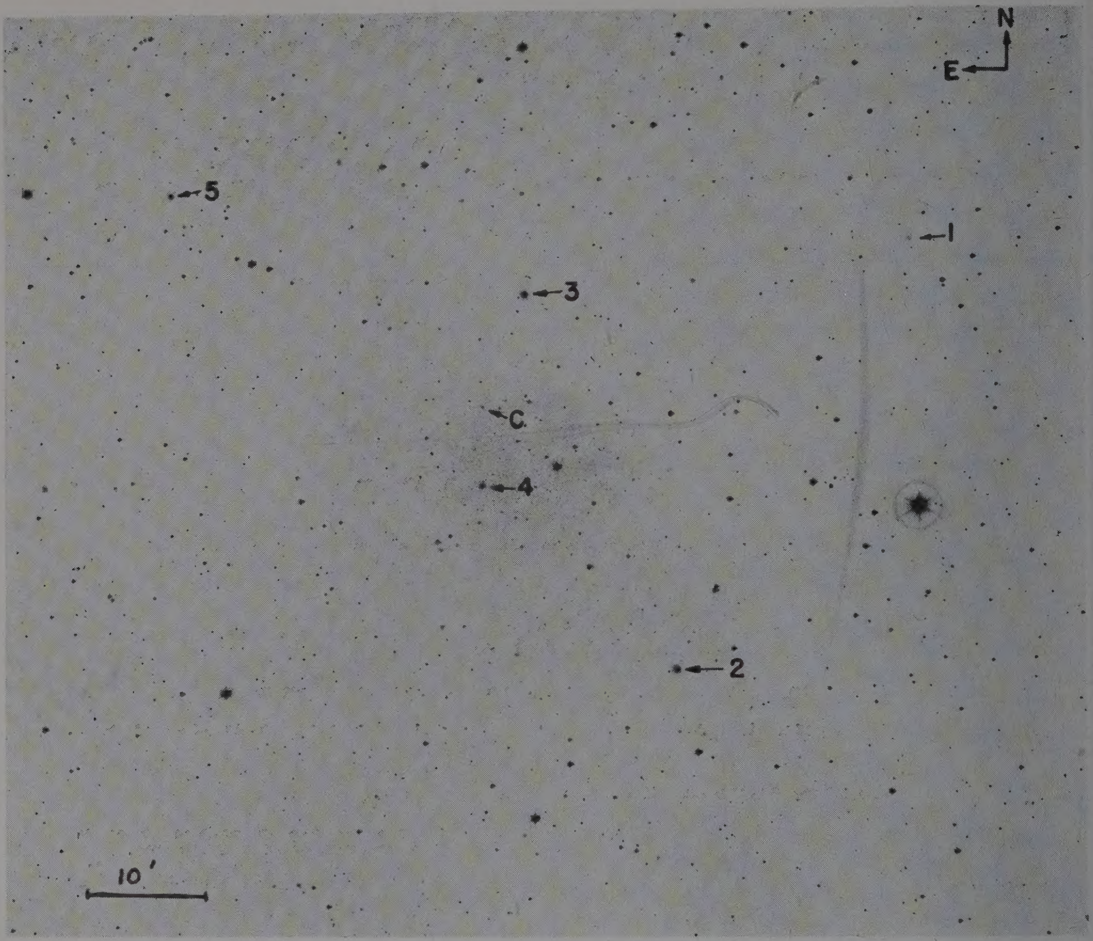

FIG. 1. The Fornax dwarf galaxy and its five globular clusters (see paper I). Photographed in the blue by the ADH Baker-Schmidt The major axis runs nearly *NE* by *SW*, and extends almost to the corners of the photograph.

II. OBSERVATIONAL DATA

Two sets of Schmidt plates have been taken of the Fornax dwarf for purposes of making star counts: one set with the ADH Schmidt at the Boyden Observatory, South Africa, and one with the 48-inch Schmidt of the Palomar Observatory. The low altitude reached by Fornax at Palomar was found to offset the advantage of the superior aperture of the 48-inch telescope, so that the ADH plates on the best nights had the smaller images and the fainter limiting magnitudes. This report is based on counts made on four ADH plates take under superior seeing conditions (Table I). Three o the plates were exposed with the 24-inch diaphrag in place, so that the vignetting-free field for these plate is 6 inches in diameter. The remaining plate, ADH 71 was exposed without the diaphragm (aperture: 3 inches) in order to reach a fainter limiting magnitude For this plate the vignetting-free field is only 2 inche in diameter. Tests made with the 24-inch aperture i place have shown that there is no systematic distanc correction within the 6-inch diameter vignetting-fre field (Hodge 1960). For plates at full aperture, the field corrections have been determined by Lindsay (1953). They are large enough that plate ADH 71 ca be used only as an approximate indicator for the oute star distribution.

TABLE I. Observational material.

Plate number	Aperture	Exposure (minutes)	Total stars counted	Background (stars per □′)
ADH 71	33-inch	75	26 600	0.70
ADH 5101	24-inch	95	12 700	0.56
ADH 5094	24-inch	90	11 100	0.52
ADH 5089	24-inch	60	9650	0.50

For the star counts a 2.5-mm grid was superimposed over the plate (scale: 68″ per mm), oriented *NS* and *EW*. The number of stars was tabulated for each square over an area extending 80 mm in each direction, with

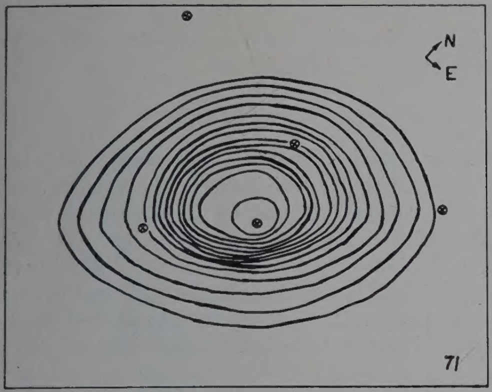

FIG. 2. Equidensity contours for plate ADH 71. Crossed circles are globular clusters. Density is in unit of stars per counting square (8 square minutes of arc). The outer contour line represents a value of 10 stars per square, and the density increases inwards in steps of 5 stars per square.

several auxiliary areas extending 40 mm further. This provided a complete count for an area of some 12 000 square millimeters, or 15 000 square minutes of arc (4.2 square degrees). Plate ADH 71 was counted three times, the remainder each counted once. Counts were made to the limiting magnitude, and each complete count was made at one long sitting. The latter was found necessary in order to avoid systematic effects. The three counts of ADH 71 agree well, and a 5% mean error represents the reliability of the count of any one square. The counts can be considered internally quite consistent.

Only the long-exposure plate, ADH 71, had images crowded together enough to make counting difficult. For the few squares at the center of the galaxy, the images on this plate were quite crowded, and the final counts uncertain. The plate ADH 5101 provided similar total counts (some 50 stars per square) at the center, but the images were smaller than for ADH 71, so that no difficulty was experienced, and the central counts for this plate can be considered reliable.

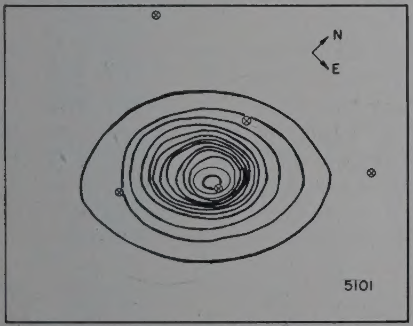

FIG. 3. Contours for plate ADH 5101. Outer line has same density as for ADH 71.

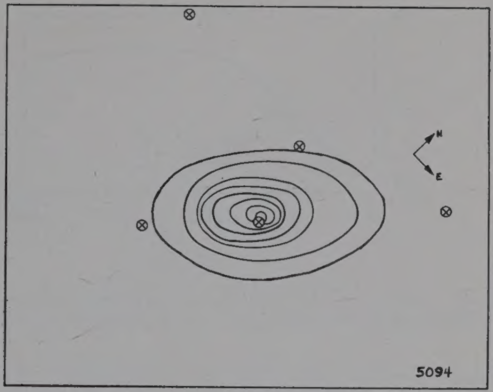

FIG. 4. Contours for plate ADH 5094. Outer line has same density as for ADH 71.

III. DISTRIBUTION OF STARS

Lines of Equidensity

In order to represent the counts graphically, equidensity contours have been constructed from the data for each plate. This was done by plotting positions of equal counts and drawing a smooth curve through all the points for $(n+2)\pm 2$, with $n=10, 15, 20\cdots$, where n is the number of stars counted per square. For example, the equidensity line for $n=15$ is as plotted actually the line for the average position of all squares with $n=15$ through $n=19$. The equidensity contour diagrams derived in this way from the four plates are shown in Figs. 2 through 5. These differ from each other somewhat in detail, but show the same general structure for the galaxy. The differences are due to the different limiting magnitudes, the certain amount of arbitrariness involved in the construction of the outermost and the innermost contours and any small irregularities in emulsion sensitivity. (The very low density gradient of the galaxy and the small steps between equidensity contours tend to exaggerate statistical fluctuations and

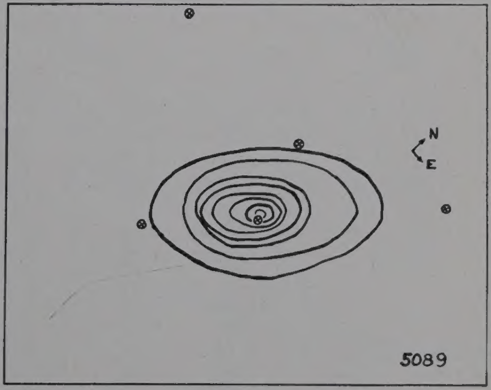

FIG. 5. Contours for plate ADH 5089. Outer line has same density as for ADH 71.

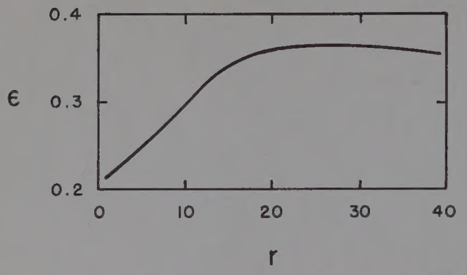

FIG. 6. Variation of the ellipticity of the Fornax galaxy with distance from the center (r is in units of minutes of arc).

irregularities far more than for isophototal maps of normal elliptical glaxies.) The counts and contours show that there are no real irregularities in the galaxy; the distribution of stars is smooth.

Orientation

The equidensity contour diagrams provide the best means of determining the orientation of the galaxy. The value obtained by averaging the orientations for all contours in Figs. 2 through 5 is 54° for the major axis, measured eastward from the north. There is no systematic change of orientation with radius, though some of the drawn contours might indicate such a situation.

Ellipticity

As in giant elliptical galaxies (Liller 1960), the ellipticity of the Fornax galaxy contours varies with the distance, increasing outwards. The ellipticity is defined here by the standard relation (Liller 1960)

$$\epsilon = 1 - (b/a), \tag{1}$$

where a is the major and b the minor axis. Figure 6 shows how the ellipticity varies with distance along the major axis. Because of the asymmetry of the galaxy, however, the ellipticities derived are not entirely realistic, and must be treated as approximate indicator of the true situation, which cannot accurately be represented by elliptical parameters.

Density Profiles

Stellar densities along the major and minor axes ar given in Table II. The values are averages for fou counting squares, reduced to the number of stars pe square minute. The area represented by each entry i Table II is 32 sq minutes, so that the statistical uncertainty of each value of the density of stars per squar minute, is $\sqrt{\rho/32}$. Major-axis density profiles are show in Figs. 7 and 8. Here it is evident that on the long exposure plate, ADH 71, saturation of images wa reached in the center of the Fornax galaxy.

For purposes of determining the distribution of star in the outermost portions of Fornax, and in th foreground, east-west profiles to greater distances from the center of the galaxy were obtained. The counts ar shown in Fig. 9, along with mean curves fitted by eye Adopted values for the density of foreground stars o each plate are given in Table I. Apparently becaus of the high galactic latitude of the Fornax dwar ($b=-64°$), there was no detectable variation of th foreground count across that portion of the plate wher counts were made.

Asymmetry

Figures 7 and 8 show that there is a striking asymmetry in the major-axis profiles, evident from all fou plates counted. This asymmetry has the characteristics of a displacement of the central, highest density poin by about 6′ from the geometrical center of the galaxy determined by the outer regions.

It is difficult to explain this asymmetry in a straightforward way. If the age of the galaxy is less than, or o the order of, the relaxation time, then the presen asymmetry might reflect the situation in the early stages of its development. The age of the galaxy i

TABLE II. Density profiles—major and minor axes.[a]

r	ADH 71				ADH 5101				ADH 5094				ADH 5089			
	Major		Minor		Major		Minor		Major		Minor		Major		Minor	
	E	W	N	S	E	W	N	S	E	W	N	S	E	W	N	S
0′	8.11	8.11	8.11	8.11	8.29	8.29	8.29	8.29	6.38	6.38	6.38	6.38	4.12	4.12	4.12	4.1
5	6.09	8.04	7.61	4.96	3.82	7.12	6.40	5.38	3.52	4.75	3.52	3.94	2.35	2.85	3.15	3.3
10	4.04	7.12	7.00	1.94	3.31	5.12	3.95	2.88	2.12	3.20	2.60	2.68	1.69	2.90	1.68	1.0
15	3.85	5.89	3.94	1.61	2.22	4.68	2.25	1.88	1.48	2.91	1.38	1.35	1.31	2.60	1.12	1.0
20	2.39	4.07	2.50	1.25	1.62	3.70	1.42	1.10	1.02	1.82	1.15	0.80	0.94	1.69	0.78	0.9
25	1.72	2.70	1.46	0.96	1.00	2.31	1.00	1.00	0.75	1.09	0.78	0.65	0.69	1.00	0.55	0.7
30	1.04	1.49	1.15	0.51	0.88	1.29	0.72	0.80	0.88	0.95	0.56	0.60	0.56	0.44	0.44	0.6
35	0.72	1.31	0.88	0.52	0.68	1.11	0.75	0.70	0.69	0.69	0.56	0.45	0.45	0.28	0.31	0.44
40	0.59	0.75	0.48	0.38	0.55	0.85	0.60	0.60	0.56	0.72	0.44	0.48	0.54	0.45		0.28
45			0.51	0.35	0.55	0.75	0.55	0.68	0.69	0.50		0.52	0.45			0.58
50			0.49	0.75	0.50	0.40	0.55	0.72		0.45		0.60				0.6
55			0.33	0.38	0.42	0.52	0.60	0.55		0.52		0.58				0.48
60			0.71	0.54			0.48	0.70		0.52		0.78				0.69
65				0.62						0.40						0.6
70				0.62						0.46						0.44

[a] Densities are given in units of stars per square minute.

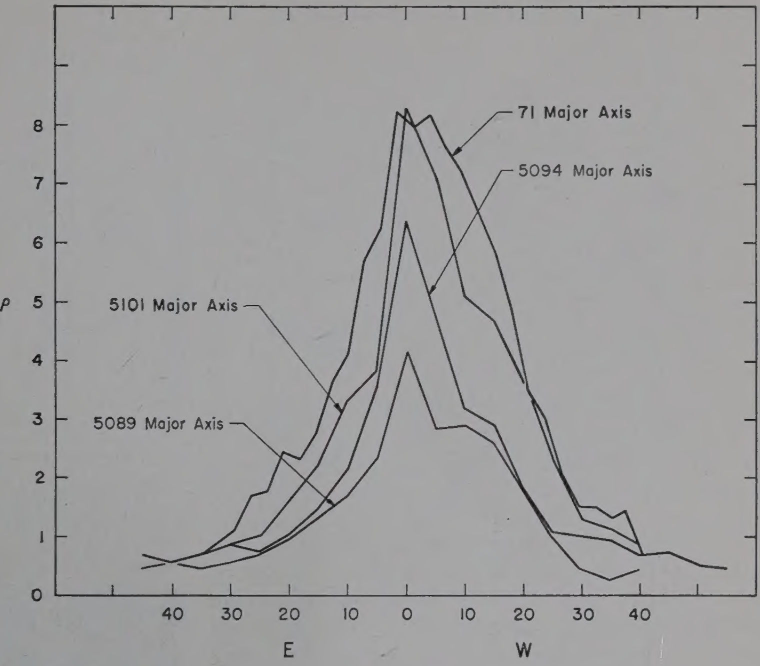

Fig. 7. Profiles for the major axis. The density ρ is in units of stars per square minute of arc; r is minutes of arc.

unknown, but probably is of the order of 10^{10} years, since its brightest stars resemble those of globular clusters. The relaxation time for stellar encounters is surely very long, but the smoothing out of large-scale density irregularities results from mixing, the characteristic time for which is much shorter. The oscillation time for a star through a galaxy of 10^7 solar masses in a 700 pc radius is of the order of 10^8 to 10^9 years, less than the age of the galaxy.

Another possibility is that there exists in the central parts of the galaxy a thin patch of dark material which obscures the point of highest density. This suggestion might be considered borne out by the fact that the deepest plate, ADH 71, shows the asymmetry least conspicuously. As has been pointed out, the central counts for this plate must be considered with reserve. Nevertheless, a dust lane such as that conspicuous near the center of NGC 185 (Baade 1944), but weaker and smaller, might account for the present observations.

A similar asymmetry along the minor axis is derived from the present data (Fig. 10), but is less marked than that for the major axis.

IV. COMPARISON WITH GIANT ELLIPTICAL GALAXIES

Mean Profile

It is of considerable interest to compare the stellar density profile of the Fornax dwarf galaxy with the luminosity profiles of giant ellipticals. The two can be directly compared if the luminosity function of the Fornax dwarf is invariant with radius, a reasonable assumption in view of the close agreement shown in Figs. 7 and 8. A mean profile for the Fornax dwarf has been constructed by smoothing the average major-axis profile of plate ADH 5094, according to the other plates' counts and the outer profiles of Fig. 9. The derived mean major-axis density distribution is given in Table III.

Hubble's Law

Hubble (1930) found that for 15 normal (giant) elliptical galaxies, the distribution of luminosity with radius could be represented well by the interpolation

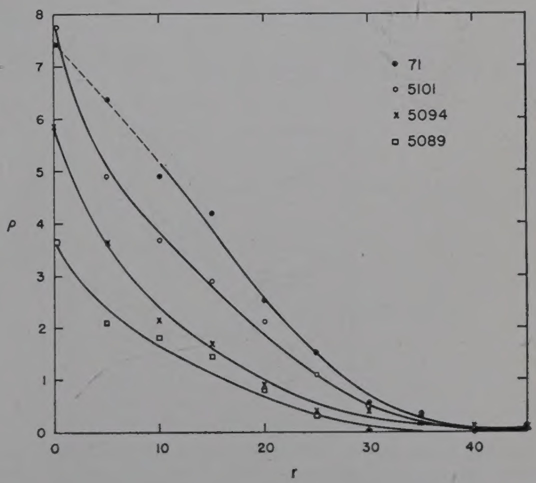

Fig. 8. Mean profiles for the major axis. Units are as for Fig. 7.

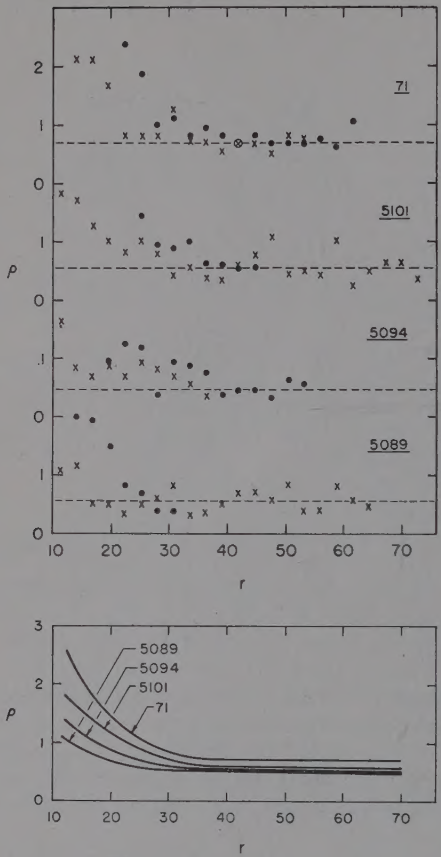

FIG. 9. Outer profiles from east-west counts. Crosses are E, circles W. Lower figure shows schematic W profiles. (ρ is in stars per square minute of arc, r is in minutes of arc.)

formula.

$$I=I_0/(r/a+1)^2 \tag{2}$$

or

$$\log I=\log I_0-2\log(r/a+1), \tag{3}$$

where I_0 is the central intensity and a is a scale parameter.

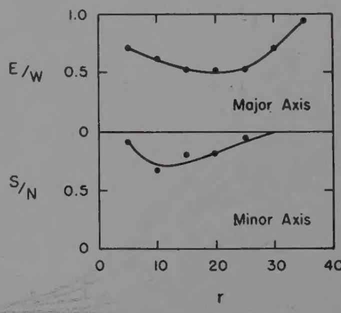

FIG. 10. Asymmetry in the Fornax galaxy. The ordinate is the ratio of the eastern to the western end of the major axis, and the ratio of the southern to the northern end of the minor axis. The abscissa is the distance in minutes of arc along the axis.

TABLE III. Major-axis profiles.

a	71	5101	5094	5089	Adopted mean[a]
	Stars per square minute				
0′	7.41	7.73	5.86	3.62	586
5	6.36	4.91	3.62	2.10	362
10	4.88	3.66	2.14	1.80	240
15	4.17	2.89	1.68	1.46	160
20	2.53	2.10	0.90	0.81	98
25	1.51	1.10	0.40	0.34	56
30	0.56	0.52	0.40	0.00	27
35	0.32	0.34	0.17	−0.14	14
40	−0.03	0.14	0.12	0.00	7
45	0.12	0.09	0.08	−0.05	1
50	0.00	−0.11	−0.07		
55	−0.05	−0.09	0.00		
60	0.03		0.00		
65			−0.12		
70			−0.06		

[a] Member stars per 100 square minutes, based on plate 5094 and smoothed with reference to the others.

The star counts of Fornax can be compared with the analogous formula

$$N=N_0/(r/a+1)^2, \tag{4}$$

where in the case of this low-density gradient galaxy N_0 can be determined, so that the proper value of a may be derived directly and the formula compared with the observations at once. Figure 11 is a plot of $\log N$ against $\log(r+a)$, which for the Hubble law produces a straight line. The value of a is calculated to be 16.2′. As Fig. 11 shows, the agreement with Hubble's formula is not unreasonable out to about $r/a=1$, beyond which the observations fall far short of the predicted densities. This can be contrasted with the case for giant ellipticals, which Hubble found to fit the interpolation formula out to values at least $r/a=20$. The fit of Fig. 11 is not improved by choosing other values for the parameters N_0 or a, so that we must conclude that the star distribution of the Fornax dwarf

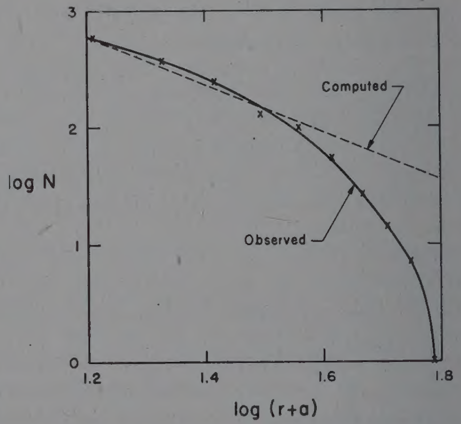

FIG. 11. A comparison of the observed distribution of stars (along the major axis) in the Fornax dwarf (crosses and solid line) with that computed from Hubble's interpolation formula. N is 100 times the density per square minute of arc (ρ).

galaxy agrees with that predicted by the Hubble law over a much smaller range than in the case of giant elliptical galaxies. The reason for this departure will be discussed in Sec. V.

de Vaucouleurs' Law

A somewhat different interpolation formula has been proposed by de Vaucouleurs (1948), who measured three elliptical galaxies and suggested that the following formula represented the data well:

$$\log(I/I_0) = -3.33\{(r/a)^{\frac{1}{4}} - 1\}, \tag{5}$$

where a is the radius within which half the light of the galaxy is emitted, and I_0 is the luminosity at a. He has since suggested that all ellipticals so far measured fit this formula better than Hubble's (de Vaucouleurs 1959).

To test the Fornax galaxy's agreement with this law, we have in Fig. 12 a plot of $\log N$ against $r^{\frac{1}{4}}$, which for de Vaucouleur's formula gives a straight line. The figure shows that there is no agreement whatever with the formula, within the distances to which observations can be carried.

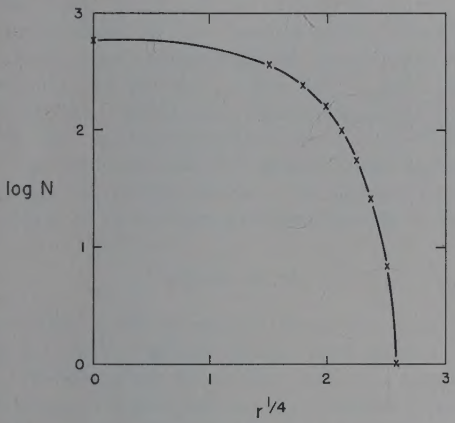

FIG. 12. The distribution of stars, plotted in units in which de Vaucouleur's luminosity distribution law makes a straight line.

V. GRAVITATIONALLY LIMITED RADIUS

As shown by von Hoerner (1957), there is a limiting radius for star clusters in the vicinity of a large mass (the Galaxy) beyond which members are lost to the cluster. It is at the point where the acceleration on the star due to the Galaxy is balanced by that due to the cluster. The expression for the gravitationally limited radius is (approximately)

$$r_s = R_g(m/2M_g)^{\frac{1}{3}}, \tag{6}$$

where R_g is the distance from the star to the Galaxy, M_g is the mass of the Galaxy, and m is the mass of the cluster. The radius thus computed has been compared with the observed radius of M15 by King (1961), and with the sizes of intergalactic tramp globular clusters by Burbidge and Sandage (1958), who point out that the appropriate value for R_g is the distance of closest approach of the object to the Galaxy, rather than necessarily the present distance.

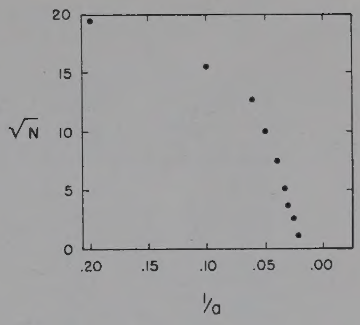

FIG. 13. The distribution of stars plotted against the reciprocal of the radius, to determine the limiting radius.

As Fig. 11 demonstrates, the star density in the Fornax galaxy falls off rather abruptly compared with the Hubble law, and it is tempting to believe that this is the result of the gravitational influence of the Galaxy on the outer stars. We may use Eq. (6), assuming reasonable values for the mass of the galaxy and its distance, to derive an approximate value for the gravitationally limited radius of the Fornax dwarf to compare with the observed radius. Similarly, we may turn the problem around to see if its observed radius confirms our rough estimate of its mass.

Adopting 188 kpc as a reasonable value for the distance of the Fornax galaxy from the Galactic center, and $1.8\times10^{11}\,M_\odot$ as a reasonable value for the mass of the Galaxy (Brandt 1960), we have left to estimate the mass of the Fornax dwarf.

One method is to compare the observed portion of the luminosity function of the galaxy, as determined from the star counts, with that for M3, for which Sandage has estimated the total mass (1954). The total

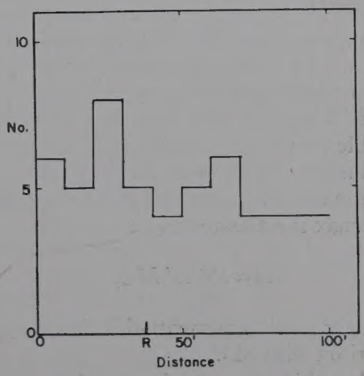

FIG. 14. The distribution of background galaxies behind the Fornax dwarf.

TABLE IV. Galaxies in the field of the Fornax dwarf.

Radius of ring	Area of ring (square minutes)	Number of galaxies in ring	Number of galaxies per 1000 sq minutes
10′	314	2	6
20′	943	5	5
30′	1570	13	8
40′	2200	11	5
50′	2827	12	4
60′	3456	18	5
70′	1000 (sector)	6	6
80′	1000 (sector)	4	4
90′	1000 (sector)	4	4
100′	1000 (sector)	4	4

number of stars (which are members of the galaxy) on plate 5101 is found to be 4295. The difference in magnitude between the brightest stars in the galaxy and the limit of the counts is not known accurately, but is estimated from measures on photoelectric sequences on other ADH plates exposed the same night and for the same length of time to be approximately 0.7 mag. (pg). For M3, Sandage (1954) finds ~50 stars in the top 0.7 mag. Thus, the comparison suggests that the galaxy has approximately 85 times the number of stars in this interval as does the globular cluster M3. If we assume the luminosity functions are the same, then we may derive a mass for Fornax by multiplying the mass of M3 (Sandage 1954) by this factor, giving

$$m \approx 1.2 \times 10^7 \, M_{\odot}.$$

It should be pointed out that, although the bright stars of Fornax do resemble globular cluster stars, there is the suggestion that the luminosity function of the galaxy is not identical to that of a typical globular cluster, either at the bright end (Hodge 1961) or the faint end (Sandage 1954).

Another estimate of the mass of Fornax, also rather uncertain, can be made from its total apparent magnitude, assuming a mass-to-light ratio. Unfortunately, both of these quantities are poorly known. The total photographic magnitude has been estimated roughly by eye to be approximately 9.0 (Shapley 1939). The mass-to-light ratios for giant ellipticals are found by Page (1959) to average approximately 30, using a Hubble constant of 75 km/sec/Mpc (Sandage 1958). However, it is probable that dwarf galaxies more nearly resemble globular clusters, which have much smaller ratios. If we adopt a mass-to-light ratio of 2 (Sandage 1954), the mass of Fornax is estimated to be

$$m \approx 2 \times 10^7 \, M_{\odot},$$

in surprisingly good agreement with that derived from the comparison with M3.

Proceeding with an assumed mass of $2 \times 10^7 \, M_{\odot}$, we derive a value of the tidal limiting radius, r_s, of 7.0 kpc. The observed radius may be determined using the method employed by King (1961). Figure 13 shows a plot of the reciprocal of the radius against $N^{\frac{1}{2}}$ (where N is the projected density of stars in units of number per square parsec). The radius obtained in this way is 56′, which is 3.3 kpc, assuming the distance of 188 kpc. Thus the observed limiting radius is approximately half the computed tidal limit, a very reasonable result, suggesting that at some time Fornax has approached the Galaxy somewhat nearer than it now lies. Its present radial velocity relative to the center of the Galaxy is −74 km/sec (Humason, Mayall, and Sandage 1956), which amounts to 74 kpc per 10^9 years, so that a closer approach during history is a very reasonable possibility.

VI. TRANSPARENCY OF THE SYSTEM

In order to check the transparency of the Fornax dwarf galaxy, to see if general internal absorption might affect the counts, a survey of background galaxies seen through the system has been made. To be sure of identification, only galaxies with decidedly elongated images were noted. All such objects were counted in circular rings of 10′ width, centered on the Fornax system. The results are given in Table V and shown in Fig. 14. As these show, the frequency of galaxies behind the Fornax dwarf (radius 56′) does not differ from that in the surrounding sky; there is probably no significant amount of general absorbing material in the galaxy.

VII. SUMMARY

The study of the distribution of the brightest stars of the Fornax dwarf galaxy has led to the following conclusions: (1) The gradient of stellar density (and luminosity density) is exceedingly small, compared to that for giant elliptical galaxies. (2) The stars in the Fornax dwarf are distributed quite smoothly, with no real irregularities detectable. (3) The major axis is oriented so that it lies 54° eastward from the north. (4) The ellipticity of the equidensity contours varies with distance, increasing from 0.21 near the center to 0.36 in the outer portions. (5) The distribution of stars near the center of the galaxy is asymmetrical; possibly a small, thin patch of absorbing material obscures part of the center. (6) The major-axis profile agrees reasonably well with the Hubble law out to $r/a=1$, beyond which the galaxy's stellar distribution falls off much more rapidly than the Hubble law. (7) There is no apparent agreement with de Vaucouleur's interpolation formula. (8) The abrupt cutoff of stars in the galaxy can be explained on the basis of the tidal limit on its radius imposed by the mass of the Galaxy. (9) The observed limiting radius of the Fornax dwarf is 3.3 kpc, assuming Baade and Hubble's (1939) distance of 188 kpc. (10) A check on the distribution of background galaxies indicates that there is no large-scale general absorption within the Fornax galaxy.

ACKNOWLEDGMENTS

Part of this work was done at the Boyden Observatory, South Africa, and at the Harvard College Observatory. I wish to thank the respective directors, Professor H. Haffner and Professor D. Menzel, for their generous help.

I am also indebted to Dr. Ivan King and to an especially helpful referee for their comments on the interpretation of the results.

REFERENCES

Baade, W. 1944, *Astrophys. J.* **100**, 147.
Baade, W. and Hubble, E. P. 1939, *Publs. Astron. Soc. Pacific* **51**, 40.
Baum, W. A. 1956, *ibid.* **67**, 328.
Brandt, J. C. 1960, *Astrophys. J.* **131**, 553.
Burbidge, E. M. and Sandage, A. R. 1958, *ibid.* **127**, 527.
Hodge, P. 1960, *ibid.* **132**, 341.
——. 1961, *Astron. J.* **66**, 83.
von Hoerner, S. 1957, *Astrophys. J.* **125**, 451.
van Houten, C. J., Oort, J. H., and Hiltner, W. A. 1954, *Astrophys. J.* **120**, 439.
Hubble, E. P. 1930, *ibid.* **71**, 131.
Humason, M. L., Mayall, N. U., and Sandage, A. R. 1956, *Astron. J.* **61**, 97.
King, I. 1961, *ibid.* **66**, 47.
Liller, M. H. 1960, *Astrophys. J.* **132**, 306.
Lindsay, E. 1953, *Irish Astron. J.* **2**, 140.
Page, T. 1959, *Astron. J.* **64**, 53.
Redman, R. O. and Shirley, E. G. 1938, *Monthly Notices Roy. Astron. Soc.* **98**, 613.
Sandage, A. R. 1954, *Astron. J.* **59**, 162.
——. 1958, *Astrophys. J.* **127**, 513.
Shapley, H. 1939, *Proc. Natl. Acad. Sci. U. S.* **25**, 565.
Sytinskaya, N. N. 1943, *Astron. J. U.S.S.R.* **20**, 54.
de Vaucouleurs, G. 1948, *Ann. d'Astrophys.* **11**, 247.
——. 1959, *Handbuch der Physik*, edited by S. Flügge (Springer-Verlag, Berlin), Vol. 53, p. 309.

THE ASTRONOMICAL JOURNAL VOLUME 66, NUMBER 6 AUGUST, 1961

The Motion of a Hyperbolic Artificial Satellite around the Oblate Earth

GEN-ICHIRO HORI
Yale University Observatory, New Haven, Connecticut
(Received May 15, 1961)

The first-order perturbation of the oblateness of the earth on the hyperbolic motion of an artificial satellite is developed by the von Zeipel method. The theory is valid for any eccentricity greater than unity and for any inclination. The modification of the Delaunay variables and the meaning of integration constants are discussed in some detail.

1. DELAUNAY VARIABLES IN HYPERBOLIC MOTION

If a stands for the distance of the perigee from the center of the hyperbola, and ae the distance between the focus and the center,

$$r=a(e^2-1)/(1+e\cos f), \tag{1}$$

where f is the true anomaly. Furthermore, n is defined by Kepler's third law, $\mu=n^2a^3$, and l by $l=nt+\text{const.}$ For convenience we call a the semimajor axis, n the mean motion, and l the mean anomaly. The notation of I for the inclination, h for the longitude of the ascending node, g for the argument of the perigee, and e for the eccentricity, corresponds to that in elliptic motion.

Let $c_j(j=1,\cdots,6)$ be a set of osculating elements. The equations of motion in these variables are

$$\sum_{j=1}^{6}[c_k,c_j]\dot{c}_j=\frac{\partial R}{\partial c_k},\quad k=1,\cdots,6$$

where R is the disturbing function, and $[c_k, c_j]$ the Lagrange brackets,

$$[p,q]=\frac{\partial(x,\dot{x})}{\partial(p,q)}+\frac{\partial(y,\dot{y})}{\partial(p,q)}+\frac{\partial(z,\dot{z})}{\partial(p,q)},$$

p, q being any pair of c_k, c_j. If (x', y'), (x'', y''), and (x''', y''') are new coordinate systems obtained successively by rotations by the angle h about the z axis, the angle I about the x' axis, and, finally, the angle g about the z'' axis, we have

$$[p,q]=[p,q]'+\frac{\partial(h,\, x'\dot{y}'-\dot{x}'y')}{\partial(p,q)},$$

$$[p,q]'=[p,q]''+\frac{\partial(I,\, y''\dot{z}''-\dot{y}''z'')}{\partial(p,q)},$$

$$[p,q]''=[p,q]'''+\frac{\partial(g,\, x'''\dot{y}'''-\dot{x}'''y''')}{\partial(p,q)},$$

or

$$[p,q]=[p,q]'''+\frac{\partial(g,G)}{\partial(p,q)}+\frac{\partial(h,H)}{\partial(p,q)},$$

if G and H are defined as in the elliptic case by

$$G=x'''\dot{y}'''+\dot{x}'''y'''=[\mu a(e^2-1)]^{\frac{1}{2}},$$

$$H=G\cos I.$$

We may evaluate $[p,q]'''$ at the perigee, where we have

$$x'''=a(e-1),\qquad y'''=0,$$

$$\dot{x}'''=0,\qquad \dot{y}'''=\left(\frac{\mu}{a}\frac{e+1}{e-1}\right)^{\frac{1}{2}},$$

$$\ddot{x}'''=-\frac{\mu}{a^2(e-1)^2},\qquad \ddot{y}'''=0.$$

Then we find

$$[p,q]'''=\sum\frac{\partial(x''',\dot{x}''')}{\partial(p,q)}$$

$$=\sum\left[\frac{\partial(x''',\dot{x}''')}{\partial(e,k)}\frac{\partial(e,k)}{\partial(p,q)}+\frac{\partial(x''',\dot{x}''')}{\partial(k,a)}\frac{\partial(k,a)}{\partial(p,q)}+\frac{\partial(x''',\dot{x}''')}{\partial(a,e)}\frac{\partial(a,e)}{\partial(p,q)}\right]$$

$$=\frac{\partial(k,C)}{\partial(p,q)}$$

if

$$l=n(t+k),$$

and

$$C=\mu/2a.$$

The canonical equations for C, k are

$$\dot{C}=\partial R/\partial k,\quad \dot{k}=-\partial R/\partial C.$$

If we use l in place of k,

$$\frac{\partial R}{\partial l}=\frac{1}{n}\frac{\partial R}{\partial k}=\frac{\dot{C}}{n}=-\frac{1}{2}\left(\frac{\mu}{a}\right)^{\frac{1}{2}}\dot{a}=\frac{d}{dt}[-(\mu a)^{\frac{1}{2}}],$$

which leads to the definition of L:

$$L=-(\mu a)^{\frac{1}{2}}.$$

Finally,

$$\dot{l}=n-\frac{\partial R}{\partial L}=\frac{\partial}{\partial L}\left(\frac{\mu^2}{2L^2}-R\right)=-\frac{\partial F}{\partial L}$$

if

$$F=-(\mu^2/2L^2)+R.$$

In summary, the relations between the Delaunay variables and Kepler's elements are

$$\begin{aligned} L&=-(\mu a)^{\frac{1}{2}}, & l&=nt+\text{const},\\ G&=[\mu a(e^2-1)]^{\frac{1}{2}}, & g&=\text{argument of the perigee},\\ H&=G\cos I, & h&=\text{longitude of the node}. \end{aligned} \tag{2}$$

The equations of motion are

$$\begin{aligned} dL/dt&=\partial F/\partial l, & dl/dt&=-\partial F/\partial L,\\ dG/dt&=\partial F/\partial g, & dg/dt&=-\partial F/\partial G,\\ dH/dt&=\partial F/\partial h, & dh/dt&=-\partial F/\partial H, \end{aligned} \tag{3}$$

with the Hamiltonian,

$$F=-(\mu^2/2L^2)+R. \tag{4}$$

In this derivation the method used by Brouwer and Clemence (1961) for the case of elliptic motion was followed. It was essential to go through the derivation in detail in order to ascertain the form of the equations in the Delaunay variables for hyperbolic motion.

2. THE DISTURBING FUNCTION

The disturbing function is

$$R=(\mu k_2/r^3)(1-3\sin^2\beta)+O(k_2^2),$$

with the equatorial plane of the earth as the reference plane and β the latitude; $\mu=k^2M$ if M is the mass of the earth, k the Gaussian constant. With the Delaunay variables, the Hamiltonian has the form

$$F=F_0+F_1+O(k_2^2),\quad F_0=-\mu^2/2L^2,$$

$$F_1=\frac{\mu^4k_2}{L^6}\left[\left(-\frac{1}{2}+\frac{3}{2}\frac{H^2}{G^2}\right)\frac{a^3}{r^3}+\left(\frac{3}{2}-\frac{3}{2}\frac{H^2}{G^2}\right)\frac{a^3}{r^3}\cos(2g+2f)\right],$$

which is of the same form as in the elliptic case except for the sign of the Keplerian term; a^3/r^3 and $(a^3/r^3)\times\cos(2g+2f)$ are understood as functions of the Delaunay variables through the Keplerian relations:

$$r=a(e\cosh u-1),\quad l=e\sinh u-u,$$

u being a parameter.

3. CANONICAL TRANSFORMATION

A canonical transformation,

$$(L,G,H,l,g,h)\rightarrow(L',G',H,l',g',h'),$$

is performed with the use of the determining function

$$S=L'l+G'g+Hh+S_1(L',G',H,l,g,-)+O(k_2^2)$$

so as to eliminate an angular variable or variables from the Hamiltonian. However, in contrast with the elliptic case where a^3/r^3 or $(a^3/r^3)\cos(2g+2f)$ consists of periodic and secular parts, there is no such distinction in the hyperbolic case. Therefore the choice of the determining function and the associated new Hamiltonian F^* is not unique as it is in the elliptic case. Different choices may result in different meaning of integration constants introduced. The choice must depend on simplicity of the development of the theory and convenience of application.

Provisionally we assume

$$F^*=F_0^*. \tag{5}$$

The energy integral

$$F=F^*$$

will then give

$$F_0^*=F_0(L')=-\mu^2/2L'^2,$$

$$\frac{\partial F_0}{\partial L'}\frac{\partial S_1}{\partial l}+F_1(L',G',H,l,g,-)=0.$$

The equation for S_1 is

$$\frac{\partial S_1}{\partial l}=-\frac{\mu^2k_2}{L'^3}\left[A\frac{a^3}{r^3}+B\frac{a^3}{r^3}\cos(2g+2f)\right], \tag{6}$$

where

$$A=-\tfrac{1}{2}+\tfrac{3}{2}(H^2/G'^2),\quad B=\tfrac{3}{2}-\tfrac{3}{2}(H^2/G'^2).$$

The new equations of motion are

$$\begin{aligned} \dot{L}'&=\partial F^*/\partial l', & \dot{l}'&=-\partial F^*/\partial L',\\ \dot{G}'&=\partial F^*/\partial g', & \dot{g}'&=-\partial F^*/\partial G',\\ \dot{H}&=\partial F^*/\partial h', & \dot{h}'&=-\partial F^*/\partial H, \end{aligned}$$

with the Hamiltonian

$$F_0^*=F_0(L')=-\mu^2/2L'^2.$$

Integration leads to the solution

$$\begin{aligned} L'&=\text{const}, & l'&=(-\mu^2/L'^3)t+l_0',\\ G'&=\text{const}, & g'&=\text{const},\\ H&=\text{const}, & h'&=\text{const}, \end{aligned}$$

with L', G', H, l_0', g', h' as six constants of integration.

4. INTEGRATION OF $\partial S_1/\partial l$

Equation (6) is integrated with use of the area integral in the form

$$\int\frac{a^3}{r^3}dl=-\frac{L}{G}\int\frac{a}{r}df=-\frac{L^3}{G^3}\int(1+e\cos f)df=-\frac{L^3}{G^3}(f+e\sin f),$$

$$\begin{aligned}\int\frac{a^3}{r^3}\cos(2g+2f)dl&=-\frac{L^3}{G^3}\int(1+e\cos f)\cos(2g+2f)df\\&=-\frac{L^3}{G^3}\left[\frac{1}{2}\sin(2g+2f)+\frac{e}{2}\sin(2g+f)+\frac{e}{6}\sin(2g+3f)\right],\end{aligned}$$

and finally we have

$$S_1=\frac{\mu^2k_2}{G'^3}\left\{A(f+e\sin f)+B\left[\frac{1}{2}\sin(2g+2f)\right.\right.$$

$$\left.\left.+\frac{e}{2}\sin(2g+f)+\frac{e}{6}\sin(2g+3f)\right]\right\}$$

$$+Z(L',G',H,g),\quad (7)$$

where Z is an arbitrary function, the introduction of which is not needed in the elliptic case in which S_1 is determined by the periodic part of F_1. The determination of Z is necessarily associated with the meaning of the constants of integration L', G', H, l_0', g', h'.

The relation between L and L' is

$$L=L'+(\partial S_1/\partial l)$$

$$=L'-\frac{\mu^2k_2}{L'^3}\left[A\frac{a^3}{r^3}+B\frac{a^3}{r^3}\cos(2g+2f)\right],$$

which shows that L' is the value of L at $r=\infty$ or $t=\pm\infty$. The meaning of the other constants should be consistent with that of L'. In order to make the problem completely defined, a choice must be made between imposing the conditions for $t=-\infty$ or $t=+\infty$. If the former is chosen, we shall have, for $t=-\infty$, the conditions

$$G'=G,\quad l'=l,\quad g'=g,\quad h'=h,\quad (8)$$

which will determine Z uniquely.

5. DETERMINATION OF $Z(L',G',H,g)$

Equation (7) leads to the relation between G and G':

$$G=G'+(\partial S_1/\partial g)$$

$$=G'+\frac{\mu^2k_2}{G'^3}B\left[\cos(2g+2f)+e\cos(2g+f)\right.$$

$$\left.+\frac{e}{3}\cos(2g+3f)\right]+\frac{\partial Z}{\partial g}.$$

Assuming the direct motion of the satellite, we have, at $t=-\infty$,

$$\cos f=-\frac{1}{e},\qquad \sin f=-\frac{(e^2-1)^{\frac{1}{2}}}{e},$$

$$\cos 2f=\frac{2-e^2}{e^2},\qquad \sin 2f=\frac{2(e^2-1)^{\frac{1}{2}}}{e^2},$$

$$\cos 3f=\frac{3e^2-4}{e^3},\qquad \sin 3f=\frac{(e^2-4)(e^2-1)^{\frac{1}{2}}}{e^3},$$

and

$$\cos(2g+2f)+e\cos(2g+f)+\frac{e}{3}\cos(2g+3f)$$

$$=\frac{\frac{2}{3}-e^2}{e^2}\cos 2g+\frac{\frac{2}{3}(e^2-1)^{\frac{3}{2}}}{e^2}\sin 2g.$$

From Eq. (8) it now follows that

$$\frac{\partial Z}{\partial g}=-\frac{\mu^2k_2}{G'^3}B\left[\frac{\frac{2}{3}-e^2}{e^2}\cos 2g+\frac{\frac{2}{3}(e^2-1)^{\frac{3}{2}}}{e^2}\sin 2g\right],$$

and integration leads to

$$Z=-\frac{\mu^2k_2}{G'^3}B\left[\frac{\frac{1}{3}-\frac{1}{2}e^2}{e^2}\sin 2g-\frac{\frac{1}{3}(e^2-1)^{\frac{3}{2}}}{e^2}\cos 2g\right]$$

$$+Z_1(L',G',H),\quad (9)$$

where Z_1 is again an arbitrary function. Substitution of Eq. (9) in Eq. (7) results in

$$S_1=\frac{\mu^2k_2}{G'^3}\left\{A(f+e\sin f)+B\left[\frac{1}{2}\sin(2g+2f)\right.\right.$$

$$+\frac{e}{2}\sin(2g+f)+\frac{e}{6}\sin(2g+3f)$$

$$\left.\left.+\frac{\frac{1}{2}e^2-\frac{1}{3}}{e^2}\sin 2g+\frac{\frac{1}{3}(e^2-1)^{\frac{3}{2}}}{e^2}\cos 2g\right]\right\}$$

$$+Z_1(L',G',H).\quad (7')$$

6. DETERMINATION OF $Z_1(L',G',H)$

The arbitrary function Z_1 will be determined by the conditions (8) after expressions for l, g, and h are obtained. Differentiation of S_1, Eq. (7′), with respect to L', G' is performed with the aid of the relations:

$$\frac{\partial\psi(e)}{\partial L}=-\frac{1}{e}\frac{G^2}{L^3}\frac{\partial\psi}{\partial e},\quad \frac{\partial\psi(e)}{\partial G}=\frac{1}{e}\frac{G}{L^2}\frac{\partial\psi}{\partial e},$$

$$\frac{\partial}{\partial e}\left(\frac{a}{r}\right)=-\frac{a^2}{r^2}\cos f,\quad \frac{\partial f}{\partial e}=-\left(\frac{a}{r}+\frac{L^2}{G^2}\right)\sin f.$$

The result is for l,

$$l'=l+(\partial S_1/\partial L')$$

$$=l+\frac{1}{e}\frac{\mu^2k_2}{L'^3G'}\left\{A\left(\frac{a^2}{r^2}\frac{G'^2}{L'^2}+\frac{a}{r}-1\right)\sin f\right.$$

$$+\frac{1}{2}B\left[\left(-\frac{a^2}{r^2}\frac{G'^2}{L'^2}-\frac{a}{r}-1\right)\sin(2g+f)\right.$$

$$+\left(\frac{a^2}{r^2}\frac{G'^2}{L'^2}\frac{a}{r}-\frac{1}{3}\right)\sin(2g+3f)-\frac{4}{3e^3}\sin 2g$$

$$\left.\left.+\frac{4+2e^2}{3e^3}\frac{G'}{L'}\cos 2g\right]\right\}+\frac{\partial Z_1}{\partial L'}.$$

The coefficient of $\frac{1}{2}B$ in the right-hand member should vanish at $t=-\infty$, since the corresponding coefficient of

B in Eq. (7′) is identically zero as a function of L', G', H, g at $t=-\infty$. Z_1 is, therefore, determined by

$$\frac{\partial Z_1}{\partial L_1'}=-\frac{1}{e}\frac{\mu^2k_2}{L'^3G'}A\frac{(e^2-1)^{\frac{1}{2}}}{e}=\frac{\mu^2k_2A}{L'^2(L'^2+G'^2)}.$$

After integration, we have

$$\begin{aligned}Z_1&=-\frac{\mu^2k_2}{G'^2}A\left(\frac{1}{L'}+\frac{1}{G'}\tan^{-1}\frac{L'}{G'}\right)+Z_2(G',H)\\&=\frac{\mu^2k_2}{G'^3}A\left[(e^2-1)^{\frac{1}{2}}+\tan^{-1}\frac{1}{(e^2-1)^{\frac{1}{2}}}\right]+Z_2(G',H),\qquad(10)\end{aligned}$$

or substitution in Eq. (7′) gives, for S_1,

$$\begin{aligned}S_1=\frac{\mu^2k_2}{G'^3}\Bigg\{&A\left[f+e\sin f+(e^2-1)^{\frac{1}{2}}+\tan^{-1}\frac{1}{(e^2-1)^{\frac{1}{2}}}\right]\\&+B\left[\frac{1}{2}\sin(2g+2f)+\frac{e}{2}\sin(2g+f)+\frac{e}{6}\sin(2g+3f)\right.\\&\left.+\left(\frac{1}{2}-\frac{1}{3e^2}\right)\sin 2g+\frac{1}{3e^2}(e^2-1)^{\frac{3}{2}}\cos 2g\right]\Bigg\}\\&+Z_2(G',H).\qquad(7'')\end{aligned}$$

7. DETERMINATION OF $Z_2(G',H)$

Differentiation of Eq. (7′) with respect to G' gives the expression for g:

$$\begin{aligned}g'&=g+(\partial S_1/\partial G')\\&=g-\frac{1}{e}\frac{\mu^2k_2}{L'^2G'^2}\Bigg\{A\left[\left(\frac{a^2}{r^2}\frac{G'^2}{L'^2}+\frac{a}{r}-1\right)\sin f-\frac{(e^2-1)^{\frac{1}{2}}}{e}\right]\\&\quad+\frac{1}{2}B\left[\left(-\frac{a^2}{r^2}\frac{G'^2}{L'^2}-\frac{a}{r}-1\right)\sin(2g+f)\right.\\&\quad+\left(\frac{a^2}{r^2}\frac{G'^2}{L'^2}+\frac{a}{r}-\frac{1}{3}\right)\sin(2g+3f)-\frac{4}{3e^3}\sin 2g\\&\quad\left.+\frac{4+2e^2}{3e^3}\frac{G'}{L'}\cos 2g\right]\Bigg\}-\frac{\mu^2k_2}{G'^4}\Bigg\{\left(-\frac{3}{2}+\frac{15}{2}\frac{H'^2}{G'^2}\right)\\&\quad\times\left[f+e\sin f+(e^2-1)^{\frac{1}{2}}+\tan^{-1}\frac{1}{(e^2-1)^{\frac{1}{2}}}\right]\\&\quad+\left(\frac{9}{2}-\frac{15}{2}\frac{H^2}{G'^2}\right)\left[\frac{1}{2}\sin(2g+2f)+\frac{e}{2}\sin(2g+f)\right.\\&\quad+\frac{e}{6}\sin(2g+3f)+\left(\frac{1}{2}-\frac{1}{3e^2}\right)\sin 2g\\&\quad\left.+\frac{1}{3e^2}(e^2-1)^{\frac{3}{2}}\cos 2g\right]\Bigg\}+\frac{\partial Z_2}{\partial G'}.\end{aligned}$$

The coefficient of B in Eq. (7″) is identically zero at $t=-\infty$, hence the coefficients of $\frac{1}{2}B$ and

$$9/2-(15/2)H^2/G'^2$$

in the above expression vanish at $t=-\infty$. The coefficient of A in Eq. (7″) is, on the other hand, expected to be identically zero or at most constant as a function of L', G' at $t=-\infty$. In fact, we see that

$$\begin{aligned}&\left[f+e\sin f+(e^2-1)^{\frac{1}{2}}+\tan^{-1}\frac{1}{(e^2-1)^{\frac{1}{2}}}\right]_{t=-\infty}\\&\qquad=\cos^{-1}\left(-\frac{1}{e}\right)+\tan^{-1}\frac{1}{(e^2-1)^{\frac{1}{2}}}=\frac{3}{2}\pi.\end{aligned}$$

Therefore the coefficients of A and $-\frac{3}{2}+(15/2)H^2/G'^2$ in the above expression are 0 and $\frac{3}{2}\pi$, respectively.

The equation for Z_2 is then

$$\frac{\partial Z_2}{\partial G'}=\frac{3}{2}\pi\frac{\mu^2k_2}{G'^4}\left(-\frac{3}{2}+\frac{15}{2}\frac{H^2}{G'^2}\right),$$

which by integration yields

$$\begin{aligned}Z_2&=\frac{3}{2}\pi\frac{\mu^2k_2}{G'^3}\left(\frac{1}{2}-\frac{3}{2}\frac{H^2}{G'^2}\right)+Z_3(H)\\&=-\frac{3}{2}\pi\frac{\mu^2k_2}{G'^3}A+Z_3(H).\end{aligned}$$

Substituting in Eq. (7″),

$$\begin{aligned}S_1=\frac{\mu^2k_2}{G'^3}\Bigg\{&A\left[f+e\sin f+(e^2-1)^{\frac{1}{2}}+\tan^{-1}\frac{1}{(e^2-1)^{\frac{1}{2}}}-\frac{3}{2}\pi\right]\\&+B\left[\frac{1}{2}\sin(2g+2f)+\frac{e}{2}\sin(2g+f)\right.\\&+\frac{e}{6}\sin(2g+3f)+\left(\frac{1}{2}-\frac{1}{3e^2}\right)\sin 2g\\&\left.+\frac{(e^2-1)^{\frac{3}{2}}}{3e^2}\cos 2g\right]\Bigg\}+Z_3(H).\end{aligned}$$

The coefficients of A and B are now identically zero at $t=-\infty$ and Z_3, an arbitrary function, is at most a constant which can be put equal to zero. The final espression for S_1 thus reduces to

$$\begin{aligned}S_1=\frac{\mu^2k_2}{G'^3}\Bigg\{&\left(-\frac{1}{2}+\frac{3}{2}\frac{H^2}{G'^2}\right)\left[f+e\sin f+(e^2-1)^{\frac{1}{2}}\right.\\&\left.+\tan^{-1}\frac{1}{(e^2-1)^{\frac{1}{2}}}-\frac{3}{2}\pi\right]+\left(\frac{3}{2}-\frac{3}{2}\frac{H^2}{G'^2}\right)\left[\frac{1}{2}\sin(2g+2f)\right.\\&+\frac{e}{2}\sin(2g+f)+\frac{e}{6}\sin(2g+3f)+\left(\frac{1}{2}-\frac{1}{3e^2}\right)\sin 2g\\&\left.+\frac{1}{3e^2}(e^2-1)^{\frac{3}{2}}\cos 2g\right]\Bigg\}.\qquad(11)\end{aligned}$$

8. SUMMARY OF THE FIRST-ORDER PERTURBATIONS

$$L=L'-\frac{\mu^2k_2}{L'^3}\left[\left(-\frac{1}{2}+\frac{3}{2}\frac{H^2}{G'^2}\right)\frac{a^3}{r^3}\right.$$
$$\left.+\left(\frac{3}{2}-\frac{3}{2}\frac{H^2}{G'^2}\right)\frac{a^3}{r^3}\cos(2g'+2f)\right],$$

$$G=G'+\frac{\mu^2k_2}{G'^3}\left(\frac{3}{2}-\frac{3}{2}\frac{H^2}{G'^2}\right)\left[\cos(2g'+2f)\right.$$
$$+e\cos(2g'+f)+\frac{e}{3}\cos(2g'+3f)$$
$$\left.+\left(1-\frac{2}{3e^2}\right)\cos 2g'+\frac{2}{3e^2}\frac{G'^3}{L'^3}\sin 2g'\right],$$

$$H=H,$$

$$l=l'-\frac{1}{e}\frac{\mu^2k_2}{L'^3G'}\left\{\left(-\frac{1}{2}+\frac{3}{2}\frac{H^2}{G'^2}\right)\right.$$
$$\times\left[\left(\frac{a^2}{r^2}\frac{G'^2}{L'^2}+\frac{a}{r}-1\right)\sin f-\frac{(e^2-1)^{\frac{1}{2}}}{e}\right]$$
$$+\left(\frac{3}{4}-\frac{3}{4}\frac{H^2}{G'^2}\right)\left[\left(-\frac{a^2}{r^2}\frac{G'^2}{L'^2}-\frac{a}{r}-1\right)\sin(2g'+f)\right.$$
$$+\left(\frac{a^2}{r^2}\frac{G'^2}{L'^2}+\frac{a}{r}-\frac{1}{3}\right)\sin(2g'+3f)$$
$$\left.\left.-\frac{4}{3e^3}\sin 2g'+\frac{4+2e^2}{3e^3}\frac{G'}{L'}\cos 2g'\right]\right\},$$

$$g=g'+\frac{1}{e}\frac{\mu^2k_2}{L'^2G'^2}\left\{\left(-\frac{1}{2}+\frac{3}{2}\frac{H^2}{G'^2}\right)\right.$$
$$\times\left[\left(\frac{a^2}{r^2}\frac{G'^2}{L'^2}+\frac{a}{r}-1\right)\sin f+\frac{G'}{eL'}\right]$$
$$+\left(\frac{3}{4}-\frac{3}{4}\frac{H^2}{G'^2}\right)\left[\left(-\frac{a^2}{r^2}\frac{G'^2}{L'^2}-\frac{a}{r}-1\right)\sin(2g'+f)\right.$$
$$+\left(\frac{a^2}{r^2}\frac{G'^2}{L'^2}+\frac{a}{r}-\frac{1}{3}\right)\sin(2g'+3f)$$
$$\left.\left.-\frac{4}{3e^3}\sin 2g'+\frac{4+2e^2}{3e^3}\frac{G'}{L'}\cos 2g'\right]\right\}$$
$$+\frac{\mu^2k_2}{G'^4}\left\{\left(-\frac{3}{2}+\frac{15}{2}\frac{H^2}{G'^2}\right)\left(f+e\sin f-\frac{G'}{L'}\right.\right.$$
$$\left.-\tan^{-1}\frac{L'}{G'}-\frac{3}{2}\pi\right)+\left(\frac{9}{2}-\frac{15}{2}\frac{H^2}{G'^2}\right)\left[\frac{1}{2}\sin(2g'+2f)\right.$$
$$+\frac{e}{2}\sin(2g'+f)+\frac{e}{6}\sin(2g'+3f)$$
$$\left.\left.+\left(\frac{1}{2}-\frac{1}{3e^2}\right)\sin 2g'-\frac{1}{3e^2}\frac{G'^3}{L'^3}\cos 2g'\right]\right\},$$

$$h=h'-\frac{3\mu^2k_2}{G'^3}\frac{H}{G'}\left\{f+e\sin f-\frac{G'}{L'}-\tan^{-1}\frac{L}{G'}-\frac{3}{2}\pi\right.$$
$$-\frac{1}{2}\sin(2g'+2f)-\frac{e}{2}\sin(2g'+f)-\frac{e}{6}\sin(2g'+3f)$$
$$\left.-\left(\frac{1}{2}-\frac{1}{3e^2}\right)\sin 2g'+\frac{1}{3e^2}\frac{G'^3}{L'^3}\cos 2g'\right\},$$

where

$$e=[(G'^2/L'^2)+1]^{\frac{1}{2}},$$

and a/r, f are the functions of e, l' through the implicit relation with u as a parameter,

$$\frac{a}{r}=\frac{1}{e\cosh u-1},\quad \cos f=\frac{e-\cosh u}{e\cosh u-1},$$
$$l'=e\sinh u-u.$$

The new mean anomaly l' is a linear function of the time

$$l'=(-\mu^2/L'^3)t+l_0' \tag{12}$$

and l_0', together with L', G', H, g', h', constitute six integration constants.

9. CONCLUDING REMARKS

The development of the theory is quite analogous to the elliptic case treated by Brouwer (1959). The essential difference is, however, seen in the meaning of the integration constants associated with the choice of the new Hamiltonian, Eq. (5). With the use of the von Zeipel method, this choice may be the most suitable, and probably unique one, for the hyperbolic case.

The essential feature of the present first-order theory may hold if the solution is extended to the second and higher orders. We may adopt the same choice for the new Hamiltonian and then the transformed Delaunay variables are constants or the same linear functions of the time, with the same meaning as in the first-order theory. In addition, as there is no separation into short-period, long-period, and secular terms, we have no critical inclination. As we cannot expect, therefore, any new theoretical feature in the higher-order theory, and as the perturbations decrease after the satellite passes its perigee, the present first-order theory may be enough both for theoretical and applicational view points.

10. MODIFICATIONS REQUIRED IN THE REPULSIVE CASE

The present theory was first developed for the case of repulsive force ($\mu<0$) in an application to the scattering problem. The results are quite similar to the present case of attractive force. The following is a summary of formulas that apply to the repulsive case:

$$r=a(e^2-1)/(e\cos f-1),\quad r=a(e\cosh u+1),$$

$$l=e\sinh u+u,\quad -\mu=n^2a^3;$$

Delaunay variables:

$$L=-[(-\mu)a]^{\frac{1}{2}},\qquad l=nt+\text{const},$$

$$G=[(-\mu)a(e^2-1)]^{\frac{1}{2}},\quad g=\text{argument of the pericenter},$$

$$H=[(-\mu)a(e^2-1)]^{\frac{1}{2}}\cos I,$$

$$h=\text{longitude of the node};$$

Hamiltonian: $F=-(\mu^2/2L^2)+R$;

Disturbing function:

$$R=-\frac{\mu^4k_2}{L^6}\left[\left(-\frac{1}{2}+\frac{3}{2}\frac{H^2}{G^2}\right)\frac{a^3}{r^3}+\left(\frac{3}{2}-\frac{3}{2}\frac{H^2}{G^2}\right)\frac{a^3}{r^3}\cos(2g+2f)\right];$$

Determining function:

$$S_1=\frac{\mu^2k_2}{G'^3}\left\{\left(-\frac{1}{2}+\frac{3}{2}\frac{H^2}{G'^2}\right)\left[f-e\sin f-(e^2-1)^{\frac{1}{2}}-\tan^{-1}\frac{1}{(e^2-1)^{\frac{1}{2}}}+\frac{\pi}{2}\right]+\left(\frac{3}{2}-\frac{3}{2}\frac{H^2}{G'^2}\right)\right.$$
$$\left.\times\left[\frac{1}{2}\sin(2g+2f)-\frac{e}{2}\sin(2g+f)-\frac{e}{6}\sin(2g+3f)+\left(\frac{1}{2}-\frac{1}{3e^2}\right)\sin 2g-\frac{(e^2-1)^{\frac{3}{2}}}{3e^2}\cos 2g\right]\right\}.$$

Comparison with Eq. (11) for the attractive case shows various changes in sign, and the change from $-\frac{3}{2}\pi$ to $+\frac{1}{2}\pi$ in the coefficient of the first part of S_1.

ACKNOWLEDGMENTS

The problem was suggested by Dr. D. Brouwer to whom I wish to express my cordial thanks for his suggestions and encouragement. The work was accomplished with the support of a contract with the Office of Naval Research.

REFERENCES

Brouwer, D. 1959, *Astron. J.* **64**, 378.
Brouwer, D. and Clemence, G. M. 1961, *Methods of Celestial Mechanics* (Academic Press Inc., New York), Chap. XI, Secs. 4 and 9.

THE ASTRONOMICAL JOURNAL VOLUME 66, NUMBER 6 AUGUST, 196

Appendix to Theoretical Evaluation of Atmospheric Drag Effects in the Motion of an Artificial Satellite

DIRK BROUWER AND GEN-ICHIRO HORI
Yale University Observatory, New Haven, Connecticut

(Received May 22, 1961)

The authors present an approximation to $\exp(-\theta)$ in powers of θ that is more convergent than a Taylor's series development if θ is limited to a given range.

In the development of our theory (Brouwer and Hori 1961), we used the Taylor's expansion for $\exp(-\alpha a x)$, where α is the coefficient of the radius vector in the exponential model of the atmosphere, a the semimajor axis, and $x=(r/a)-1$. Since the expansion is not effective when $|\alpha a x|$ takes values greater than unity, we suggested in the paper to use the approximation of the form

$$e^{-\theta}=A_0-A_1\theta+\frac{A_2}{2}\theta^2-\frac{A_3}{6}\theta^3+\frac{A_4}{24}\theta^4-\frac{A_5}{120}\theta^5,$$

where the coefficients A_j may be determined by the principle of the least square when a range of θ is given, say, $-\gamma\leq\theta\leq+\gamma$.

For simplicity let C_j be

$$C_j=(-1)^j(A_j/j!),\quad j=0,1,\cdots,5;$$

the evaluation of C_j is then formulated by the equation

$$I=\int_{-\gamma}^{\gamma}e^{-(\theta+\gamma)}[e^{-\theta}-\sum_{j=0}^{5}C_j\theta^j]^2d\theta=\text{minimum},\qquad(1)$$

where $\exp[-(\theta+\gamma)]$ is a provisional weight function taking the value 1 at the perigee $(\theta=-\gamma)$ and $\exp(-2\gamma)$ at the apogee $(\theta=+\gamma)$.

The conditions

$$\partial I/\partial C_j=0,\quad j=0,1,\cdots,5,$$

lead to the normal equations for C_j

$$\sum_{j=0}^{5}C_j\int_{-\gamma}^{\gamma}\theta^{j+k}e^{-(\theta+\gamma)}d\theta=\int_{-\gamma}^{\gamma}\theta^k e^{-(2\theta+\gamma)}d\theta,\qquad k=0,1,\cdots,5.\qquad(2)$$

Evaluation of the integrals results in

$$\int_{-\gamma}^{\gamma}\theta^j e^{-(2\theta+\gamma)}d\theta=\frac{j!}{2^{j+1}}\left[e^{\gamma}\sum_{k=0}^{j}\frac{2^k}{k!}(-\gamma)^k-e^{-3\gamma}\sum_{k=0}^{j}\frac{2^k}{k!}\gamma^k\right],\qquad j=0,1,\cdots,5,$$

and

$$\int_{-\gamma}^{\gamma}\theta^j e^{-(\theta+\gamma)}d\theta=j!\left[\sum_{k=0}^{j}\frac{1}{k!}(-\gamma)^k-e^{-2\gamma}\sum_{k=0}^{j}\frac{1}{k!}\gamma^k\right],\qquad j=0,1,\cdots,10.$$

If Q_j, Q_j' $(j=0,1,\cdots,5)$, and P_j, P_j' $(j=0,1,\cdots,10)$ are defined by

$$\begin{aligned}&Q_0=1,\quad Q_j=Q_{j-1}+(-1)^j(2^j/j!)\gamma^j,\\&Q_0'=1,\quad Q_j'=Q_{j-1}'+(2^j/j!)\gamma^j;\quad j=1,2,\cdots,5,\\&P_0=1,\quad P_j=P_{j-1}+(-1)^j(1/j!)\gamma^j,\\&P_0'=1,\quad P_j'=P_{j-1}'+(1/j!)\gamma^j;\quad j=1,2,\cdots,10,\end{aligned}\qquad(3)$$

and b_j, a_{jk} by

$$\begin{aligned}&b_j=\frac{j!}{2^{j+1}}(Q_je^{\gamma}-Q_j'e^{-3\gamma}),&&j=0,1,\cdots,5,\\&a_j=j!(P_j-P_j'e^{-2\gamma});&&j=0,1,\cdots,10,\\&a_{jk}=a_{j+k},&&j,k=0,1,\cdots,5,\end{aligned}\qquad(4)$$

the normal equations are

$$\sum_{k=0}^{5}a_{jk}C_k=b_j,\quad j=0,1,\cdots,5.\qquad(5)$$

The formulas (3), (4) show a method of evaluation of the integrals appearing in the normal equations (2).

The normal equations (5) were solved for five cases, $\gamma=1,2,\cdots,5$ with the use of the IBM 650 and IBM 610. The resulting values of A_j are given in Table I.

TABLE I. The coefficients A'_j for $\gamma=1,2,\cdots,5$ and their mean errors.

γ	1	2	3	4	5
A_0	+0.9999900	+0.9972809	+0.9927548	+0.7834172	−1.0892184
A_1	+0.9966676	+1.0143125	+1.0874261	+1.5197473	+2.8373974
A_2	+1.0002082	+1.0054912	+0.9636549	+1.1811823	+3.2873689
A_3	+1.0840814	+0.8701602	+0.6360486	−0.4107438	−3.4678006
A_4	+1.0209843	+1.0931240	+1.3336037	+1.3402296	+0.2884029
A_5	−0.3977536	+1.7402653	+2.0209304	+3.2974657	+6.0651410
μ	0.00058	0.0039	0.018	0.12	0.55
μ_0	0.0006	0.027	0.35	2.3	11

The mean error μ is evaluated by

$$\mu^2=I/(1-e^{-2\gamma}),$$

where I is the integral defined in Eq. (1).

If we put

$$B_{2j}=C_j^2+2\sum_{k=1} C_{j-k}C_{j+k}, \quad j=0, 1, \cdots, 5,$$

$$B_{2j+1}=2\sum_{k=0} C_{j-k}C_{j+k+1}, \quad j=0, 1, \cdots, 4,$$

the C's under the summation being limited to C_0, C_1, $\cdots$, C_5, we have

$$\begin{aligned} I=&\int_{-\gamma}^{\gamma} e^{-(3\theta+\gamma)}d\theta-2\sum_{j=0}^{5} C_j\int_{-\gamma}^{\gamma} \theta^j e^{-(2\theta+\gamma)}d\theta \\ &+\sum_{j=0}^{10} B_j\int_{-\gamma}^{\gamma} \theta^j e^{-(\theta+\gamma)}d\theta \\ =&\tfrac{1}{3}(e^{2\gamma}-e^{-4\gamma})-2\sum_{j=0}^{5} C_jb_j+\sum_{j=0}^{10} B_ja_j. \end{aligned}$$

For a comparison, the mean error μ_0 is calculated in the case of the Taylor's expansion ($A_j=1$, $j=0$, $1, \cdots, 5$):

$$\mu_0{}^2=\frac{1}{2\gamma}\int_{-\gamma}^{\gamma}\left[e^{-\theta}-\left(1-\theta+\frac{1}{2}\theta^2-\frac{1}{6}\theta^3+\frac{1}{24}\theta^4-\frac{1}{120}\theta^5\right)\right] d\theta.$$

The results for μ, μ_0 are shown in Table I for the five cases, $\gamma=1, 2, \cdots, 5$.

ACKNOWLEDGMENTS

This investigation was supported by the National Aeronautics and Space Administration. It is a pleasure to acknowledge our indebtedness to Dr. Y. Kozai. Discussions with him on the possible divergence of developments that arise in the drag theory of artificial satellites led to the procedure developed in this paper. We also extend our thanks to Mr. W. Wilkinson, staff member of the Yale University Computing Center, for aid with programming on the IBM 650.

THE ASTRONOMICAL JOURNAL VOLUME 66, NUMBER 6 AUGUST, 196

The Orbit of Comet Schwassmann-Wachmann 1

Paul Herget
Cincinnati Observatory, Cincinnati, Ohio

(Received April 3, 1961)

A numerical integration and orbit correction for Comet Schwassmann-Wachmann 1925 II reveals the existence of nongravitational forces acting upon the comet. The comet approaches within 1 a.u. of Jupiter in 1974, and drastic changes in the elements will be produced. Extended opposition ephemerides are furnished until 1973.

The Comet Schwassmann-Wachmann 1925 II is a uniquely peculiar object in the solar system because of the sporadic large increases in brightness which occur without any known explanation. To provide the observers with adequate ephemerides, a set of orbital elements was established (Herget 1947), based on observations extending from 1934 to 1944. Subsequent ephemerides have been published on *Harvard Announcement Cards*. An extension of this work has now been undertaken by means of the standard IBM 650 electronic computer programs which are in regular use at the University of Cincinnati for the determination of minor planet orbits.

Nearly 200 observations of the comet were selected haphazardly from the literature with the view to covering rather uniformly the entire observed arc. The resulting orbit correction gave residuals in right ascension which are shown in the upper part of Fig. 1. There are systematic deviations in excess of ten seconds of arc. Every plotted point was included in the least-squares solution, although several outstanding points are of doubtful validity. The declination residuals are not shown.

A second solution was then computed, excluding those points which are marked off by a dashed curve, as shown in the lower part of Fig. 1. The residuals of this solution are shown in Table I. The amplitude of the systematic deviations is reduced to about three seconds of arc, and there appears to be a sharp discontinuity near JD 2426000. It may be assumed for the present that lesser discontinuities, which have not been resolved, exist at other points. If we adopt a residual of 20″ in the mean anomaly at JD 2425200, this is equivalent to a change of 0″.025 in the daily mean motion, corresponding to an impulsive change in the velocity of the comet of one meter per second. The previous orbit (Herget 1947) had not shown any evidence of such deviation from gravitational motion, but it may be seen from Fig. 1 that this was entirely fortuitous.

In the future, the comet approaches Jupiter within 2.0 a.u. during the interval from JD 2440960 = 1971 Jan. 9 to JD 2443600 = 1978 April 2, with a minimum of less than 1.0 a.u. near JD 2442220 = 1974 June 22. The nature of the changes in the osculating elements may be seen from Table II. After the close approach to Jupiter, the eccentricity is diminished to about half its present value, and the period is diminished to such an extent that there is not another close approach to Jupiter for nearly a century. It is not intended to imply that these are accurate prediction elements, since other sporadic changes may occur, and the perturbation computations are not entirely adequate at the 20-day interval which has been used. However, the printed ephemerides (Table III) may be expected to be reasonably reliable for practical purposes.

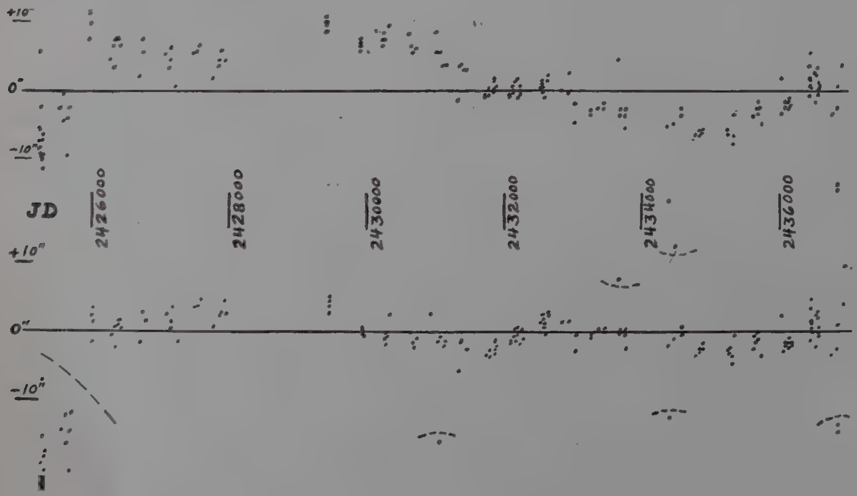

Fig. 1. Upper part: residuals in right ascension. Lower part: residuals from second solution.

TABLE I. Residuals.

JDE−2400000	$\cos\delta\,\Delta\alpha$	$\Delta\delta$	$\cos\delta\,\Delta\alpha$	$\Delta\delta$	Place
252 09.7	−15″.3	− 4″.6	(−22″.3)	(− 6″.9)	Lick
252 10.5	−14.3	− 4.0	(−21.2)	(− 6.3)	Yerk
252 12.6	−12.2	− 4.5	(−19.2)	(− 6.8)	Yerk
252 15.6	−15.9	− 8.3	(−22.8)	(−10.6)	Yerk
252 15.7	−15.1	− 7.8	(−22.0)	(−10.1)	Yerk
252 28.6	−16.4	− 9.7	(−23.0)	(−12.0)	Yerk
252 29.6	−14.9	− 4.6	(−21.5)	(− 6.8)	Lick
252 29.7	−16.2	− 5.4	(−22.8)	(− 7.6)	Lick
252 23.6	− 8.9	− 9.5	(−15.4)	(−11.8)	Yerk
252 35.6	− 0.6	− 5.9	(− 7.1)	(− 8.1)	Yerk
252 43.6	−15.6	− 4.0	(−22.1)	(− 6.1)	Yerk
252 43.7	−15.4	− 5.6	(−21.8)	(− 7.8)	Yerk
252 56.5	−16.1	− 4.3	(−22.1)	(− 6.3)	Lick
252 58.6	−16.1	− 4.4	(−22.1)	(− 6.4)	Yerk
252 63.6	−15.2	− 3.7	(−21.1)	(− 5.6)	Lick
252 66.6	−15.6	− 4.6	(−21.4)	(− 6.6)	Lick
252 67.5	−17.2	− 6.5	(−23.0)	(− 8.4)	Yerk
252 86.6	−12.9	− 5.5	(−18.3)	(− 7.2)	Lick
252 87.7	−15.0	− 3.6	(−20.4)	(− 5.3)	Lick
252 89.5	−12.2	− 3.6	(−17.6)	(− 5.3)	Yerk
252 97.5	−12.9	− 6.0	(−18.1)	(− 7.6)	Yerk
255 38.8	−10.5	− 1.5	(−14.4)	(− 1.3)	Lick
255 89.7	− 8.1	− 2.2	(−12.2)	(− 2.3)	Lick
255 91.7	−12.2	+ 3.3	(−16.3)	(+ 3.2)	Yerk
256 23.6	−16.7	− 1.8	(−20.5)	(− 2.0)	Yerk
256 25.6	−11.1	− 3.9	(−14.9)	(− 4.1)	Yerk
256 78.5	− 9.0	− 0.4	(−12.0)	(− 0.5)	Yerk
259 73.6	− 0.9	− 1.7	− 1.8	− 0.9	Yerk
259 75.6	+ 3.1	−11.5	+ 2.1	−10.8	Yerk
259 99.5	+ 4.1	+ 5.7	+ 3.1	+ 6.3	Yerk
259 99.5	+ 2.1	+ 2.1	+ 1.2	+ 2.7	Yerk
262 71.9	− 2.4	0.0	− 0.8	+ 0.2	Yerk
263 03.7	− 1.2	+ 2.8	+ 0.5	+ 2.9	Yerk
263 03.7	− 4.5	+ 4.1	− 2.8	+ 4.3	Yerk
263 38.8	− 0.8	+ 2.0	+ 0.9	+ 2.2	Yerk
263 83.7	− 0.1	− 3.4	+ 1.4	− 3.2	Yerk
263 93.7	0.0	− 9.6	+ 1.5	− 9.4	Yerk
264 10.6	− 1.0	+ 1.2	+ 0.4	+ 1.3	Yerk
266 90.8	− 5.3	+ 0.4	− 1.9	− 0.6	Yerk
267 34.6	− 0.5	+ 2.4	+ 2.9	+ 1.4	Yerk
267 74.6	− 1.7	+ 2.3	+ 1.4	+ 1.4	Yerk
270 78.8	− 1.9	+13.1	+ 2.5	+10.8	Yerk
271 06.8	− 4.2	+ 7.1	+ 0.2	+ 4.8	Yerk
271 21.6	− 3.0	+ 3.4	+ 1.4	+ 1.2	Yerk
271 55.6	− 0.9	+ 1.8	+ 3.3	− 0.3	Yerk
272 06.6	− 5.5	+ 2.8	− 1.7	+ 0.8	Yerk
274 83.7	− 1.6	+ 3.0	+ 3.3	− 0.3	Yerk
275 06.7	− 1.5	+ 3.6	+ 3.5	+ 0.3	Yerk
275 65.6	+ 0.4	+ 9.5	+ 4.8	+ 6.5	Yerk
277 56.9	− 3.5	+ 3.2	+ 0.7	+ 0.3	Yerk
278 36.9	− 2.8	+ 3.3	+ 2.1	− 0.3	Yerk
278 59.7	− 2.3	+ 3.9	+ 2.8	+ 0.1	McD
278 99.6	− 0.7	+ 4.6	+ 4.3	+ 0.9	McD
279 26.6	− 2.2	+ 5.8	+ 2.6	+ 2.2	Yerk
294 27.3	+ 3.7	− 0.1	+ 3.8	− 0.7	Joh
294 28.7	+ 2.6	− 1.4	+ 2.8	− 2.0	Yerk
294 29.5	+ 4.8	+ 0.7	+ 5.0	+ 0.1	Cord
294 32.5	+ 4.1	+ 1.5	+ 4.2	+ 0.9	Cord
299 01.5	+ 3.3	+ 1.8	+ 0.9	+ 0.8	McD
299 04.6	+ 2.2	+ 0.8	− 0.2	− 0.2	Lick
299 04.7	+ 2.7	+ 1.8	+ 0.3	+ 0.8	Lick
299 28.6	+ 1.9	0.0	− 0.5	− 0.9	McD
302 33.7	+ 3.3	+ 3.5	− 1.0	+ 1.4	Yerk
302 48.6	+ 2.3	+ 2.6	− 1.9	+ 0.5	Yerk
302 49.6	+ 4.1	− 1.1	− 0.1	− 3.1	Yerk
302 63.6	+ 3.3	+ 1.2	− 0.8	− 0.8	McD
303 11.5	+ 5.9	+ 4.9	+ 2.3	+ 3.2	McD
306 08.7	+ 3.9	+ 2.0	− 0.1	+ 0.3	McD
306 46.6	+ 2.4	+ 1.4	− 1.7	− 0.3	McD
306 76.6	+ 1.7	− 0.5	− 2.1	− 2.0	Yerk
307 01.6	+ 2.5	+ 0.4	− 1.0	− 1.0	Yerk
309 05.8	+ 4.8	+ 2.1	+ 2.7	+ 1.8	Yerk
310 18.6	−13.5	− 6.1	(−16.0)	− 6.2	McD
310 25.7	+ 1.1	+ 0.3	− 1.4	+ 0.2	McD
310 74.5	+ 1″.5	−19″.8	− 0″.8	(−20″.0)	Yerk
311 10.5	0.0	− 4.7	− 2.0	− 4.8	Yerk
311 39.5	+ 0.2	− 1.2	− 1.5	− 1.3	Yerk
313 20.8	− 5.9	− 6.6	− 5.8	− 5.8	Yerk
313 55.7	− 1.7	− 1.2	− 1.4	− 0.3	Yerk
313 85.9	− 1.5	− 2.4	− 1.2	− 1.4	McD
314 14.6	− 2.4	− 1.7	− 2.3	− 0.6	McD
314 38.5	− 2.2	− 2.7	− 2.2	− 1.7	Yerk
317 07.9	− 5.7	− 0.3	− 3.2	+ 0.4	Lick
317 08.0	− 5.6	− 0.1	− 3.1	+ 0.6	Lick
317 73.0	− 5.6	− 2.1	− 2.6	− 1.2	Lick
317 73.0	− 6.5	− 2.1	− 3.5	− 1.2	Lick
318 45.6	− 5.8	− 0.3	− 3.1	+ 0.6	Lick
318 45.7	− 5.4	− 0.1	− 2.7	+ 0.8	Lick
318 52.6	− 4.1	− 0.4	− 1.4	+ 0.5	Lick
318 52.7	− 3.7	− 0.7	− 1.1	+ 0.2	Lick
318 80.6	− 4.7	− 1.5	− 2.1	− 0.7	Lick
318 80.7	− 4.7	− 1.1	− 2.1	− 0.3	Lick
320 98.9	− 6.2	+ 1.6	− 1.6	+ 1.2	Lick
320 98.9	− 5.9	+ 2.0	− 1.3	+ 1.5	Lick
321 17.9	− 5.5	+ 0.2	− 0.6	− 0.2	Lick
321 18.8	− 4.7	+ 1.2	+ 0.2	+ 0.7	Lick
321 51.7	− 6.4	+ 2.4	− 1.2	+ 1.9	Lick
321 51.8	− 4.7	+ 1.7	+ 0.5	+ 1.3	Lick
321 74.8	− 4.8	+ 0.4	+ 0.5	0.0	Lick
321 74.8	− 5.8	+ 0.4	− 0.4	0.0	Lick
322 07.5	− 7.1	+ 2.0	− 1.9	+ 1.8	Yerk
322 56.7	− 4.4	+ 0.6	+ 0.3	+ 0.4	Lick
322 86.7	− 5.5	+ 0.1	− 1.0	− 0.3	Lick
322 86.7	− 5.6	− 0.2	− 1.1	− 0.5	Lick
325 01.9	− 4.8	+ 3.6	+ 1.4	+ 1.5	Lick
325 02.0	− 4.8	+ 3.5	+ 1.4	+ 1.4	Lick
325 38.9	− 4.1	+ 2.7	+ 2.6	+ 0.5	Lick
325 39.0	− 4.8	+ 2.1	+ 1.9	− 0.1	Lick
325 64.7	− 5.5	+ 0.7	+ 1.3	− 1.4	Lick
325 64.8	− 6.2	+ 1.1	+ 0.7	− 1.0	Lick
325 98.7	− 6.9	+ 1.2	− 0.2	− 0.7	Lick
326 14.7	− 4.2	+ 1.7	+ 2.2	− 0.1	Yerk
326 14.8	− 3.6	+ 1.8	+ 2.9	0.0	Yerk
328 26.9	− 4.7	+ 3.5	+ 1.4	+ 0.6	McD
329 24.9	− 6.0	+ 4.6	+ 1.6	+ 0.8	Yerk
329 46.6	− 2.9	+ 7.4	+ 4.8	+ 3.6	Yerk
330 09.6	−10.0	+ 1.1	− 2.9	− 2.3	Lick
330 37.7	− 7.0	+ 3.1	− 0.3	− 0.1	Lick
332 50.9	− 8.0	+ 4.9	− 0.9	+ 0.5	Lick
332 51.0	− 7.6	+ 4.7	− 0.5	+ 0.3	Lick
333 49.7	− 7.8	+ 4.8	+ 0.3	− 0.2	Lick
333 49.7	− 7.9	+ 5.1	+ 0.2	+ 0.1	Lick
334 20.7	− 7.1	+ 5.0	0.0	+ 0.6	Lick
334 20.7	− 6.7	+ 4.9	+ 0.4	+ 0.5	Lick
336 54.9	− 0.1	+ 5.7	+ 7.7	+ 0.5	McD
336 86.9	− 8.6	+ 5.9	− 0.4	+ 0.3	Lick
336 86.9	− 7.9	+ 5.8	+ 0.3	+ 0.2	Lick
337 42.8	− 8.0	+ 5.0	+ 0.3	− 0.7	Lick
337 42.8	− 8.9	+ 5.4	− 0.6	− 0.3	Lick
337 71.6	−10.2	+ 2.0	− 2.4	− 3.5	Yerk
343 70.0	− 8.9	+ 3.0	− 2.0	− 0.9	McD
343 94.9	−19.9	+ 4.7	(−12.7)	+ 0.8	McD
344 56.8	− 9.4	+ 5.7	− 1.0	+ 1.2	Yerk
344 74.7	+ 3.8	+ 5.1	(+12.3)	+ 0.4	Yerk
345 61.6	− 6.6	+ 5.0	+ 0.9	+ 0.5	Yerk
345 62.7	− 7.7	+ 4.9	− 0.2	+ 0.4	Lick
347 78.0	−10.0	+ 2.4	− 3.4	+ 0.1	McD
348 05.9	− 9.5	+ 3.4	− 2.4	+ 1.1	Lick
348 06.0	−10.1	+ 2.6	− 3.0	+ 0.4	Lick
348 61.8	−10.3	+ 1.9	− 2.3	− 0.8	Lick
348 61.8	− 9.7	+ 2.3	− 1.7	− 0.3	Lick
352 21.9	− 8.7	+ 0.6	− 2.8	+ 0.5	McD
352 52.8	− 9.4	+ 1.4	− 3.1	+ 1.2	Lick
352 52.9	− 8.6	+ 1.2	− 2.4	+ 1.0	Lick
353 00.7	−11.1	− 1.3	− 4.8	− 1.9	Lick
353 00.7	− 9.9	− 0.6	− 3.7	− 1.2	Lick
353 30.7	− 6.4	−15.0	− 0.5	(−15.6)	Lick
356 00.9	− 5.6	− 1.1	− 2.3	− 0.1	McD

TABLE I (*continued*)

JDE−2400000	cosδ Δα	Δδ	cosδ Δα	Δδ	Place
356 66.7	− 4″7	+ 0″8	− 0″9	+ 1″8	Lick
356 66.8	− 5.4	+ 0.5	− 1.7	+ 1.5	Lick
356 88.7	− 3.7	+ 0.4	0.0	+ 1.4	Lick
356 88.8	− 4.9	+ 0.8	− 1.1	+ 1.7	Lick
357 19.6	− 6.9	− 2.4	− 3.4	− 1.6	Yerk
360 19.8	+ 0.6	+ 2.3	+ 2.1	+ 3.4	Yerk
360 43.8	− 4.6	+ 6.1	− 2.9	+ 7.3	Yerk
360 71.8	− 3.3	− 0.2	− 1.5	+ 1.0	Lick
360 71.8	− 3.8	− 0.1	− 2.1	+ 1.1	Lick
360 73.7	− 3.1	+ 0.5	− 1.3	+ 1.7	McD
361 05.7	− 3.2	+ 1.3	− 1.6	+ 2.4	Lick
361 05.8	− 4.1	+ 1.7	− 2.4	+ 2.8	Lick
361 06.5	− 2.6	+ 0.4	− 1.0	+ 1.5	Yerk
361 39.6	− 3.1	+ 1.1	− 1.7	+ 2.1	Yerk
361 53.5	− 3.4	− 2.1	− 2.0	− 1.1	Yerk
364 27.8	− 2.4	+ 0.7	− 1.1	+ 2.1	McD
364 29.8	+ 0.4	+ 2.9	+ 1.7	+ 4.3	Yerk
364 29.8	+ 2.2	+ 3.4	+ 3.4	+ 4.8	Yerk
364 30.9	− 0.8	+ 0.4	+ 0.5	+ 1.9	McD
364 31.9	+ 0″1	+ 0″7	+ 1″4	+ 2″1	McD
364 38.8	+ 3.6	+ 2.9	+ 4.9	+ 4.3	Yerk
364 58.6	+ 0.1	− 2.9	+ 1.3	− 1.4	Yerk
364 68.8	− 1.2	+ 3.2	+ 0.1	+ 4.7	Yerk
365 07.5	+ 1.2	+ 2.8	+ 2.3	+ 4.3	Yerk
365 19.6	− 3.2	+ 0.2	− 2.1	+ 1.6	Yerk
365 36.5	+ 1.0	+ 1.6	+ 2.0	+ 3.0	Yerk
365 39.5	− 1.9	+ 0.5	− 0.8	+ 1.9	Yerk
365 43.5	− 1.2	− 2.4	− 0.2	− 1.0	Yerk
365 46.5	+ 1.8	− 1.3	+ 2.8	+ 0.1	Yerk
365 49.5	− 0.3	+ 6.0	+ 0.7	+ 7.3	Yerk
365 78.5	− 0.5	− 2.3	+ 0.4	− 1.1	Yerk
367 59.8	− 5.1	− 3.4	− 3.2	− 1.8	Yerk
368 12.8	− 4.5	− 3.1	− 2.2	− 1.1	McD
368 13.8	−16.0	− 0.1	(−13.7)	+ 1.9	McD
368 14.7	−17.0	− 1.9	(−14.6)	+ 0.1	McD
368 19.9	− 1.4	− 0.6	+ 1.0	+ 1.5	McD
369 01.6	+ 1.8	+11.9	+ 4.0	(+14.1)	Yerk
369 32.5	+ 7.6	− 2.2	+ 9.6	− 0.2	Yerk

TABLE II. Orbital elements.

Epoch	JD 2430000.5=1941 Jan 6ᵈ0 ET				
M_0	353°57207		(1950.0)	P	Q
n	0.06103951	ω	356°22229	+0.74633139	+0.65774613
a	6.3884541	Ω	322.00326	−0.60620675	+0.60863191
e	0.13550168	i	9.51656	−0.27477780	+0.44377609

Epoch	JD 2436000.5			Epoch	JD 2442000.5		
M_0	1°79256		(1950.0)	M_0	354°89931		(1950.0)
n	0.06120884	ω	355°81213	n	0.06498197	ω	13°38059
a	6.376666	Ω	321.60963	a	6.127377	Ω	319°66031
e	0.13156612	i	9.48662	e	0.11077967	i	9.75739
Epoch	JD 2440000.5			Epoch	JD 2443000.5		
M_0	244°36047		(1950.0)	M_0	59°82706		(1950.0)
n	0.6058729	ω	356°78453	n	0.06871720	ω	26°46438
a	6.420203	Ω	321.57133	a	5.903273	Ω	314.98038
e	0.13164292	i	9.46211	e	0.06984021	i	9.12152
Epoch	JD 2441000.5			Epoch	JD 2444000.5		
M_0	302°58791		(1950.0)	M_0	123°39207		(1950.0)
n	0.06123687	ω	0°57024	n	0.06747432	ω	40°06428
a	6.374720	Ω	320.90788	a	5.975544	Ω	313.34247
e	0.13585640	i	9.46080	e	0.06249733	i	9.25203

TABLE III. Opposition ephemerides, 1960–1973.

	α (1950.0)	δ	ρ	r
960–61				
un 15	2^{h} $47^{m}5$	+24° 49′	6.958	6.185
25	2 54.2	+25 26		
ul 5	3 00.4	+26 02	6.758	6.203
15	3 06.0	+26 36		
25	3 10.9	+27 07	6.504	6.221
ug 4	3 15.1	+27 37		
14	3 18.3	+28 03	6.218	6.240
24	3 20.5	+28 27		
ep 3	3 21.6	+28 48	5.926	6.258
13	3 21.6	+29 04		
23	3 20.4	+29 16	5.662	6.276
ct 3	3 18.1	+29 22		
13	3 14.8	+29 23	5.461	6.294
23	3 10.7	+29 17		
ov 2	3 06.0	+29 06	5.357	6.313
12	3 01.0	+28 49		
22	2 56.2	+28 28	5.371	6.331
ec 2	2 51.8	+28 04		
12	2 48.0	+27 39	5.506	6.349
22	2 45.2	+27 14		
an 1	2 43.5	+26 52	5.743	6.368
11	2 42.9	+26 34		
21	2 43.4	+26 19	6.049	6.386
31	2 45.1	+26 10		
eb. 10	2 47.9	+26 06	6.387	6.404
20	2 51.6	+26 06		
Mar 2	2 56.2	+26 11	6.719	6.422
12	3 01.6	+26 21		
22	3 07.6	+26 32	7.015	6.440
Var	+3.2	+13		
1961–62				
Jul 20	4 38.0	+30 31	7.222	6.547
30	4 44.4	+30 49		
Aug 9	4 50.2	+31 07	6.988	6.564
19	4 55.2	+31 24		
29	4 59.4	+31 40	6.709	6.581
Sep 8	5 02.6	+31 56		
18	5 04.8	+32 11	6.410	6.598
28	5 05.8	+32 24		
Oct 8	5 05.7	+32 36	6.124	6.615
18	5 04.3	+32 46		
28	5 01.9	+32 53	5.886	6.632
Nov 7	4 58.4	+32 56		
17	4 54.1	+32 55	5.733	6.649
27	4 49.2	+32 50		
Dec 7	4 44.0	+32 40	5.694	6.666
17	4 39.0	+32 26		
27	4 34.3	+32 10	5.779	6.682
Jan 6	4 30.4	+31 52		
16	4 27.3	+31 33	5.977	6.699
26	4 25.4	+31 14		
Feb 5	4 24.7	+30 57	6.259	6.715
15	4 25.2	+30 42		
25	4 26.8	+30 29	6.588	6.731
Mar 7	4 29.5	+30 20		
17	4 33.2	+30 13	6.925	6.747
27	4 37.8	+30 09		
Apr 6	4 43.1	+30 06	7.238	6.762
16	4 49.1	+30 05		
26	4 55.7	+30 05	7.499	6.778
Var	+3.1	+3		
1962–63				
Aug 4	6 10.8	+30 24	7.609	6.852
14	6 17.3	+30 25		
24	6 23.3	+30 27	7.389	6.866
Sep 3	6 28.6	+30 29		
13	6 33.1	+30 32	7.115	6.880
23	6 36.8	+30 36		
Oct 3	6 39.5	+30 41	6.811	6.894
13	6 41.2	+30 47		
23	6 41.8	+30 54	6.509	6.908

	α (1950.0)	δ	ρ	r
1962–63				
Nov 2	6^{h} $41^{m}2$	+31° 02′		
12	6 39.5	+31 09	6.244	6.921
22	6 36.7	+31 17		
Dec 2	6 33.0	+31 23	6.056	6.935
12	6 28.5	+31 27		
22	6 23.6	+31 29	5.976	6.948
Jan 1	6 18.5	+31 27		
11	6 13.6	+31 22	6.021	6.960
21	6 09.2	+31 14		
31	6 05.5	+31 04	6.186	6.973
Feb 10	6 02.8	+30 52		
20	6 01.1	+30 39	6.445	6.985
Mar 2	6 00.6	+30 25		
12	6 01.2	+30 12	6.761	6.997
22	6 02.9	+29 58		
Apr 1	6 05.6	+29 45	7.097	7.009
11	6 09.2	+29 33		
21	6 13.7	+29 21	7.417	7.020
May 1	6 18.8	+29 09		
11	6 24.6	+28 57	7.692	7.032
Var	+2.8	−5		
1963–64				
Aug 19	7 33.9	+26 41	7.895	7.084
29	7 40.1	+26 27		
Sep 8	7 45.8	+26 15	7.685	7.094
18	7 50.9	+26 04		
28	7 55.4	+25 55	7.414	7.104
Oct 8	7 59.1	+25 47		
18	8 01.9	+25 42	7.105	7.113
28	8 03.8	+25 40		
Nov 7	8 04.7	+25 41	6.790	7.122
17	8 04.6	+25 44		
27	8 03.4	+25 50	6.505	7.130
Dec 7	8 01.2	+25 57		
17	7 58.1	+26 06	6.290	7.139
27	7 54.2	+26 15		
Jan 6	7 49.7	+26 24	6.180	7.147
16	7 45.0	+26 32		
26	7 40.3	+26 37	6.194	7.155
Feb 5	7 35.9	+26 39		
15	7 32.0	+26 39	6.330	7.162
25	7 28.9	+26 36		
Mar 6	7 26.8	+26 30	6.567	7.170
16	7 25.7	+26 22		
26	7 25.6	+26 11	6.871	7.177
Apr 5	7 26.6	+25 59		
15	7 28.5	+25 45	7.201	7.183
25	7 31.3	+25 30		
May 5	7 34.9	+25 14	7.522	7.190
15	7 39.2	+24 56		
25	7 44.2	+24 36	7.805	7.196
Var	+2.4	−11		
1964–65				
Sep 22	8 57.9	+19 44	7.866	7.227
Oct 2	9 02.7	+19 22		
12	9 07.0	+19 03	7.597	7.231
22	9 10.5	+18 46		
Nov 1	9 13.3	+18 32	7.284	7.235
11	9 15.2	+18 22		
21	9 16.3	+18 16	6.959	7.239
Dec 1	9 16.4	+18 14		
11	9 15.5	+18 16	6.658	7.242
21	9 13.7	+18 21		
31	9 11.0	+18 30	6.422	7.245
Jan 10	9 07.5	+18 41		
20	9 03.6	+18 54	6.287	7.248
30	8 59.2	+19 07		
Feb 9	8 54.8	+19 19	6.275	7.250
19	8 50.6	+19 30		

TABLE III (*continued*)

		α (1950.0)	δ	ρ	r
1965					
Mar	1	$8^h\,46^m9$	+19° 38′	6.386	7.252
	11	8 43.8	+19 43		
	21	8 41.5	+19 45	6.603	7.254
	31	8 40.1	+19 43		
Apr	10	8 39.6	+19 38	6.892	7.255
	20	8 40.1	+19 30		
	30	8 41.5	+19 18	7.213	7.257
May	10	8 43.8	+19 04		
	20	8 46.8	+18 46	7.533	7.258
	30	8 50.6	+18 26		
Jun	9	8 54.9	+18 03	7.818	7.258
	19	8 59.7	+17 38		
	29	9 05.0	+17 11	8.047	7.258
	Var	+2.1	−14		
1965–66					
Oct	7	10 02.9	+11 44	7.932	7.256
	17	10 07.5	+11 14		
	27	10 11.5	+10 46	7.665	7.254
Nov	6	10 15.0	+10 21		
	16	10 17.8	+10 00	7.349	7.252
	26	10 19.7	+09 43		
Dec	6	10 20.9	+09 31	7.016	7.250
	16	10 21.1	+09 23		
	26	10 20.4	+09 20	6.703	7.248
Jan	5	10 18.9	+09 22		
	15	10 16.5	+09 29	6.449	7.245
	25	10 13.4	+09 40		
Feb	4	10 09.7	+09 54	6.291	7.242
	14	10 05.7	+10 10		
	24	10 01.6	+10 27	6.254	7.239
Mar	6	9 57.6	+10 43		
	16	9 53.9	+10 58	6.342	7.236
	26	9 50.8	+11 11		
Apr	5	9 48.5	+11 20	6.537	7.232
	15	9 46.9	+11 25		
	25	9 46.2	+11 25	6.809	7.228
May	5	9 46.5	+11 22		
	15	9 47.6	+11 14	7.121	7.223
	25	9 49.5	+11 02		
Jun	4	9 52.2	+10 46	7.435	7.219
	14	9 55.6	+10 26		
	24	9 59.5	+10 02	7.722	7.214
Jul	4	10 04.0	+09 35		
	14	10 08.9	+09 06	7.956	7.208
	Var	+1.9	−16		
1966–67					
Oct	22	11 04.7	+02 48	7.889	7.178
Nov	1	11 09.4	+02 11		
	11	11 13.5	+01 37	7.626	7.171
	21	11 17.0	+01 06		
Dec	1	11 19.9	+00 38	7.310	7.163
	11	11 22.0	+00 13		
	21	11 23.4	−00 04	6.972	7.156
	31	11 23.8	−00 18		
Jan	10	11 23.4	−00 26	6.648	7.148
	20	11 22.1	−00 29		
	30	11 19.9	−00 26	6.377	7.140
Feb	9	11 17.1	−00 17		
	19	11 13.6	−00 04	6.197	7.132
Mar	1	11 09.7	+00 13		
	11	11 05.7	+00 32	6.133	7.123
	21	11 01.8	+00 53		
	31	10 58.1	+01 13	6.193	7.114
Apr	10	10 55.0	+01 31		
	20	10 52.5	+01 46	6.364	7.105
	30	10 50.8	+01 58		
May	10	10 50.0	+02 05	6.616	7.096
	20	10 50.0	+02 07		
	30	10 50.9	+02 04	6.915	7.086

		α (1950.0)	δ	ρ	r
1967					
Jun	9	$10^h\,52^m6$	+01° 56′		
	19	10 55.1	+01 43	7.224	7.076
	29	10 58.3	+01 26		
Jul	9	11 02.1	+01 04	7.511	7.066
	19	11 06.4	+00 38		
	29	11 11.2	+00 08	7.751	7.055
	Var	+1.9	−18		
1967–68					
Nov	6	12 08.1	−06 38	7.748	6.999
	16	12 13.0	−07 19		
	26	12 17.5	−07 58	7.494	6.987
Dec	6	12 21.5	−08 35		
	16	12 24.8	−09 08	7.184	6.975
	26	12 27.3	−09 37		
Jan	5	12 29.1	−10 02	6.845	6.962
	15	12 29.9	−10 22		
	25	12 29.9	−10 37	6.511	6.949
Feb	4	12 28.9	−10 45		
	14	12 27.0	−10 48	6.233	6.937
	24	12 24.4	−10 44		
Mar	5	12 21.0	−10 34	6.017	6.923
	15	12 17.2	−10 19		
	25	12 13.2	−10 00	5.922	6.910
Apr	4	12 09.1	−09 38		
	14	12 05.3	−09 14	5.948	6.896
	24	12 01.9	−08 51		
May	4	11 59.2	−08 30	6.087	6.882
	14	11 57.3	−08 13		
	24	11 56.2	−07 59	6.314	6.868
Jun	3	11 55.9	−07 50		
	13	11 56.6	−07 47	6.596	6.854
	23	11 58.2	−07 50		
Jul	3	12 00.5	−07 57	6.898	6.840
	13	12 03.6	−08 10		
	23	12 07.4	−08 29	7.186	6.825
Aug	2	12 11.8	−08 52		
	12	12 16.7	−09 19	7.435	6.810
	Var	+2.1	−18		
1968–69					
Dec	10	13 29.3	−17 24	7.292	6.717
	20	13 34.1	−18 03		
	30	13 38.2	−18 40	6.994	6.701
Jan	9	13 41.6	−19 13		
	19	13 44.2	−19 43	6.659	6.684
	29	13 45.9	−20 09		
Feb	8	13 46.6	−20 29	6.320	6.668
	18	13 46.3	−20 45		
	28	13 44.9	−20 54	6.014	6.651
Mar	10	13 42.7	−20 57		
	20	13 39.6	−20 54	5.777	6.634
	30	13 35.8	−20 44		
Apr	9	13 31.6	−20 29	5.642	6.617
	19	13 27.3	−20 09		
	29	13 23.0	−19 46	5.624	6.600
May	9	13 19.1	−19 22		
	19	13 15.8	−18 57	5.722	6.583
	29	13 13.3	−18 34		
Jun	8	13 11.7	−18 14	5.916	6.566
	18	13 11.0	−17 58		
	28	13 11.3	−17 47	6.176	6.548
Jul	8	13 12.5	−17 42		
	18	13 14.7	−17 42	6.468	6.531
	28	13 17.8	−17 48		
Aug	7	13 21.6	−17 59	6.759	6.513
	17	13 26.1	−18 15		
	27	13 31.3	−18 36	7.019	6.495
Sep	6	13 37.1	−19 00		
	16	13 43.3	−19 28	7.227	6.477
	Var	+2.5	−18		

TABLE III (*continued*)

	α (1950.0)	δ	ρ	r
969–70				
Dec 25	$14^{\mathrm{h}}\ 55^{\mathrm{m}}.2$	−25° 33′	7.050	6.386
Jan 4	15 01.4	−26 08		
14	15 07.1	−26 41	6.774	6.368
24	15 12.1	−27 13		
Feb 3	15 16.2	−27 43	6.453	6.350
13	15 19.3	−28 09		
23	15 21.4	−28 33	6.114	6.331
Mar 5	15 22.4	−28 53		
15	15 22.3	−29 10	5.791	6.313
25	15 21.0	−29 21		
Apr 4	15 18.6	−29 27	5.521	6.294
14	15 15.1	−29 27		
24	15 11.0	−29 21	5.337	6.276
May 4	15 06.4	−29 10		
14	15 01.6	−28 53	5.263	6.257
24	14 56.8	−28 32		
Jun 3	14 52.6	−28 09	5.305	6.238
13	14 48.9	−27 45		
23	14 46.3	−27 21	5.454	6.220
Jul 3	14 44.5	−26 59		
13	14 44.0	−26 41	5.683	6.201
23	14 44.5	−26 27		
Aug 2	14 46.2	−26 17	5.960	6.183
12	14 48.9	−26 12		
22	14 52.6	−26 12	6.252	6.164
Sep 1	14 57.2	−26 16		
11	15 02.6	−26 24	6.529	6.146
21	15 08.8	−26 36		
Oct 1	15 15.6	−26 51	6.765	6.127
Var	+3.3	−13		
1971				
Jan 29	16 55.9	−30 56	6.568	6.018
Feb 8	17 02.8	−31 14		
18	17 08.9	−31 31	6.273	6.001
28	17 14.1	−31 47		
Mar 10	17 18.4	−32 03	5.945	5.983
20	17 21.5	−32 18		
30	17 23.4	−32 32	5.613	5.965
Apr 9	17 24.0	−32 46		
19	17 23.3	−32 57	5.312	5.948
29	17 21.3	−33 06		
May 9	17 18.1	−33 12	5.075	5.931
19	17 14.0	−33 14		
29	17 09.1	−33 11	4.933	5.914
Jun 8	17 03.9	−33 04		
18	16 58.6	−32 52	4.904	5.897
28	16 53.6	−32 37		
Jul 8	16 49.3	−32 18	4.988	5.880
18	16 45.9	−31 58		
28	16 43.6	−31 38	5.171	5.863
Aug 7	16 42.6	−31 19		
17	16 42.8	−31 01	5.423	5.847
27	16 44.3	−30 45		
Sep 6	16 47.1	−30 32	5.713	5.831
16	16 51.0	−30 21		
26	16 55.9	−30 12	6.006	5.815
Oct 6	17 01.8	−30 05		
16	17 08.6	−30 00	6.275	5.799
26	17 16.1	−29 56		
Nov 5	17 24.2	−29 52	6.495	5.784
Var	+4.0	−3		
1972				
Feb 13	$18^{\mathrm{h}}\ 57^{\mathrm{m}}.3$	−28° 45′	6.421	5.711
23	19 05.5	−28 35		
Mar 4	19 13.0	−28 25	6.171	5.697
14	19 19.8	−28 15		
24	19 25.8	−28 08	5.871	5.683
Apr 3	19 30.8	−28 03		
13	19 34.7	−27 59	5.547	5.670
23	19 37.5	−27 57		
May 3	19 39.0	−27 59	5.227	5.657
13	19 39.3	−28 03		
23	19 38.3	−28 08	4.944	5.645
Jun 2	19 36.0	−28 15		
12	19 32.6	−28 22	4.732	5.633
22	19 28.3	−28 28		
Jul 2	19 23.3	−28 33	4.618	5.621
12	19 18.0	−28 36		
22	19 12.8	−28 35	4.619	5.609
Aug 1	19 07.9	−28 31		
11	19 03.8	−28 23	4.733	5.598
21	19 00.7	−28 13		
31	18 58.7	−28 00	4.941	5.587
Sep 10	18 58.0	−27 45		
20	18 58.7	−27 28	5.214	5.577
30	19 00.7	−27 09		
Oct 10	19 03.8	−26 50	5.516	5.567
20	19 08.1	−26 30		
30	19 13.4	−26 08	5.816	5.558
Nov 9	19 19.6	−25 44		
19	19 26.6	−25 19	6.084	5.548
Var	+4.2	+15		
1973				
Mar 19	21 09.7	−18 19	6.180	5.502
29	21 16.9	−17 42		
Apr 8	21 23.4	−17 07	5.930	5.496
18	21 29.3	−16 34		
28	21 34.3	−16 04	5.635	5.490
May 8	21 38.5	−15 38		
18	21 41.6	−15 16	5.320	5.484
28	21 43.7	−14 59		
Jun 7	21 44.6	−14 47	5.013	5.479
17	21 44.5	−14 40		
27	21 43.1	−14 39	4.745	5.475
Jul 7	21 40.6	−14 42		
17	21 37.2	−14 50	4.551	5.471
27	21 33.1	−15 01		
Aug 6	21 28.3	−15 13	4.458	5.467
16	21 23.3	−15 25		
26	21 18.5	−15 37	4.482	5.464
Sep 5	21 14.1	−15 47		
15	21 10.5	−15 53	4.619	5.461
25	21 07.8	−15 55		
Oct 5	21 06.3	−15 54	4.849	5.458
15	21 06.0	−15 48		
25	21 06.9	−15 36	5.139	5.456
Nov 4	21 08.9	−15 20		
14	21 12.1	−14 59	5.455	5.455
24	21 16.3	−14 34		
Dec 4	21 21.4	−14 04	5.763	5.454
14	21 27.3	−13 30		
24	21 33.8	−12 53	6.035	5.453
Var	+3.7	+28		

The variation given at the end of each opposition ephemeris is the variation-per-ten-days for each coordinate in the neighborhood of the opposition. The residuals in the left-hand columns of Table I represent the deviations from the preliminary orbit. The right-hand columns give the representation of each observation from the adopted solution. Each residual enclosed in parentheses ( ) was excluded from the final least-squares solution.

REFERENCE

Herget, P. 1947, *Astron. J.* **53**, 16.

THE ASTRONOMICAL JOURNAL VOLUME 66, NUMBER 6 AUGUST, 1961

Parallax and Orbital Motion of 42 Comae = ADS 8804 from Plates Taken with the 24-Inch Sproul Refractor

SARAH LEE LIPPINCOTT
Sproul Observatory, Swarthmore College, Swarthmore, Pennsylvania

(Received May 4, 1961)

Measurement and reduction of plates taken with the Sproul refractor over the interval 1920–1959 yield $+''.038\pm''.005$ (p.e.) for the relative parallax and $+''.008\pm''.010$ (p.e.) for the semi-axis major of the photocentric orbit of 42 Comae. The relative mass of the B component is $.507\pm.014$ (p.e.), whereas the individual masses are poorly determined due to the small value of the parallax: $M_A=1.6\ \odot$. $M_B=1.7\ \odot$ each with a p.e. of $\pm.45\ \odot$.

THE visual binary 42 Comae = ADS 8804, $13^h5.1^m$, $+18°3'$ (1900) has a period $25^y.83$ and semi-axis major $''.672$ (Pavel 1949). The combined visual magnitude is 4.30 and the $\Delta m_{pv}=.02$ according to Eggen (1956). The spectrum is F4, Mt. Wilson classification; the radial velocity is −17.7 km/sec (Wilson 1953). The inclination of the orbit is close to 90°, the greatest separation never exceeds $0''.6$, so that the image of AB always appears circular on the Sproul photographs.

The procedure described in previous Sproul publications has been followed (van de Kamp and Lippincott 1949). A total of 999 exposures on 300 plates covering 98 nights with a total weight 208 were measured by Mrs. Mary Jackson on the St. Clair-Kasten measuring machine. The brightness of 42 Comae was reduced 6.7 mag. by means of a rotating sector to equal the average magnitude of the reference system of three stars.

Table I gives information about the reference stars as well as the dependences for 1940 and their annual changes. The coordinates of the standard frame and of 42 Comae hold for the approximate epoch 1940.

The nightly means were represented by the equations of conditions

$$X=c_x+\mu_x t+\pi P_\alpha+\alpha Q_\alpha,$$

$$Y=c_y+\mu_y t+\pi P_\delta+\alpha Q_\delta,$$

where the symbols have the usual meaning; t is counted from 1940.000.

The orbital factors were computed from Pavel's (1949) orbit:

$$P=25^y.83,\quad i=89°.94,$$

$$e=.494,\quad \omega=278°.58,$$

$$T=1911.61,\quad \Omega\doteq 11°.93.$$

Separate solutions in right ascension and declination yield the following results (the scale factor is 1 mm $=18''.87$):

$$\begin{array}{lllll}
 & \text{mm} & & \text{p.e.} & \text{wt} \\
c_x= & -3.59069 & & & \\
c_y= & +4.29875 & & & \\
\mu_x= & -0.0220270 & =-0''.415649 & \pm 0''.000808 & 5894 \\
\mu_y= & +0.0085943 & =+0.162174 & \pm 0.000530 & 5971 \\
\pi_x= & +0.002131 & =+0.04021 & \pm 0.00723 & 73.62 \\
\pi_y= & +0.002322 & =+0.04383 & \pm 0.00804 & 26.12 \\
\alpha_x= & -0.01691 & =-0.3191 & \pm 0.0574 & 1.16 \\
\alpha_y= & +0.00121 & =+0.0228 & \pm 0.0077 & 26.34 \\
\text{p.e. } 1_x= & \pm 0.0033 & =\pm 0.062 & & \\
\text{p.e. } 1_y= & \pm 0.0022 & =\pm 0.041 & &
\end{array}$$

A least-squares solution for π and α was made combining the material in right ascension and declination with the following results:

$$\begin{array}{llll}
 & \text{mm} & \text{p.e.} & \text{wt} \\
c_x= & -3.5902 & & \\
c_y= & +4.29876 & & \\
\mu_x= & -0''.41903 & \pm 0''.00047 & 12202 \\
\mu_y= & +0.16286 & \pm 0.00066 & 6126 \\
\alpha= & +0.0082 & \pm 0.0097 & 27.55 \\
\pi= & +0.0375 & \pm 0.0054 & 90.54 \\
\text{p.e. } 1= & \pm 0.0513 & &
\end{array}$$

While the extent of the reference configuration is large in right ascension, it does not fully account for

TABLE I. Reference stars.

No.	Diameter	m_{pv}	Spectrum	x_s	y_s	Dep. 1940	ΔD/year
	mm			mm	mm		
1	.093	11.3	G0	−76.37	− 1.73	.395	+.00025
2	.104	11.1	K0	+25.57	−15.53	.166	−.00041
3	.099	11.2	F8	+50.80	+17.26	.439	+.00016
42 Com	.110	(10.98)	F4	− 3.59	+ 4.30		

TABLE II. Normal points of residuals.

Epoch	Number of nights	Total weight	v_x unit .0001 mm	v_y
1921.22	5	3	+ 7	−10
22.80	6	3½	−36	+ 8
26.67	4	3	−67	+25
38.91	4	5	− 2	− 3
40.64	4	7	+10	− 3
43.91	4	8	+43	+ 5
46.85	9	19½	+15	0
48.97	8	21	+16	−16
51.01	5	12	− 6	−10
52.25	5	12	−21	+ 8
53.32	5	13	+ 2	+13
54.21	7	17	− 1	− 6
55.87	12	32	0	0
57.23	6	13	−27	+16
58.24	9	27	0	0
59.18	5	12	− 7	− 3

the large value of the probable error of unit weight given by the least-squares solution (Lippincott 1957). Table II gives normal points of the residuals found from the combined solution. These residuals also show greater scatter in right ascension than in declination.

This solution for parallax supersedes the early Sproul determination (Pitman 1928), which was based on part of the present material. The reduction to absolute is made in the usual manner (Lippincott 1958) and leads to $\pi_{\mathrm{abs}}=+0''.042\pm0''.005$. Combined with the values for the other published determinations (Jenkins 1952) the weighted mean value for the absolute parallax is $+0''.051\pm0''.004$. With this value, the semi-axis major a becomes 13 ± 1 a.u., yielding $M_A+M_B=3.3\pm0.8\odot$, the p.e. in both cases arising solely from the p.e. of the parallax. Adopting Eggen's value $\Delta m=0.02$, $\beta=0.495$; we derive the mass ratio

$$B=(\alpha/a)+\beta=+0.507\pm0.014 \text{ (p.e.)}$$

taking into account only the p.e. of α (van de Kamp 1945).

Thus we find $M_A=1.6\odot$, $M_B=1.7\odot$ each with a p.e. $=\pm0.45\odot$ due to the large percentage error in the parallax. The absolute visual magnitudes of the two components are 3.58 and 3.60, the absolute bolometric magnitudes 3.53 and 3.55. Considering the probable errors of the masses, the two components do not deviate from the mass-luminosity relation.

Pavel's orbit gives $i=89°56'\pm6'$. For eclipses to take place the inclination would have to be within 1′ of 90°. Assuming for the moment this to be the case, the next eclipse would occur very close to periastron lasting roughly two hours; the uncertainty of the parameters precludes a more accurate timing of smallest angular separation so that without continuous 24-hour observations for several days the occurrence or absence of an eclipse could not be established.

ACKNOWLEDGMENT

This investigation was partially supported by a grant from the National Science Foundation.

REFERENCES

Eggen, O. J. 1956, *Astron. J.* **61**, 371.
Jenkins, L. F. 1952, *General Catalogue of Trigonometric Stellar Parallaxes* (Yale University Observatory, New Haven, Connecticut).
Lippincott, S. L. 1957, *Astron. J.* **62**, 61.
——. 1958, *ibid.* **63**, 230.
Pavel, F. 1949, *Astron. Nach.* **277**, 153.
Pitman, J. H. 1928, *Sproul Obs. Publ.* **10**, 68.
van de Kamp, P. 1945, *Astron. J.* **51**, 161.
van de Kamp, P. and Lippincott, S. L. 1949, *ibid.* **55**, 16.
Wilson, R. E. 1953, *General Catalogue of Stellar Radial Velocities* (Carnegie Institution of Washington, Washington, D. C.).

THE ASTRONOMICAL JOURNAL VOLUME 66, NUMBER 6 AUGUST, 196

NOTICES

Observing Time on Kitt Peak

THE Kitt Peak National Observatory was established to provide American astronomers and qualified graduate students with modern telescopic and instrumental equipment for astronomical research. Also, the Board of Directors of AURA (Association of Universities for Research in Astronomy) has set the policy that about 60% of the observing time on Kitt Peak shall be made available to visiting astronomers and graduate students.

No charge is made for telescope time, but visiting astronomers will be billed for food and lodging while working on Kitt Peak.

At the present time, two moderate-sized, Cassegrain focus telescopes are in operation on Kitt Peak: a 16-inch and a 36-inch. Auxiliary equipment consists of photoelectric photometers for both telescopes, and a grating spectrograph for the 36-inch.

Since a number of inquiries and requests for observing time have already been received, an *Observers' Information Leaflet* and an *Observing Time Request Form* have been prepared for those persons who are interested in using the Kitt Peak facilities. Copies may be obtained by writing to: Office of the Director, Kitt Peak National Observatory, 950 North Cherry Avenue, Tucson, Arizona.

It is AURA policy that observing-time requests be granted on the basis of scientific merit of the proposed program. In most cases, the Observatory staff reviews proposals and makes recommendations regarding assignments; occasionally, the advice of outside referees may be sought. Visiting astronomers are expected to do their own observing on Kitt Peak, although they may bring a qualified assistant if their program requires it.

Subject to existing Federal regulations, qualified foreign astronomers may use the Observatory's facilities. In cases of U.S. and foreign programs judged to be of equal merit, however, preference will be given to astronomers resident in the U.S., because of the national character of the Observatory.

To the extent that funds are available, the Observatory's graduate student program pays for travel and subsistence expenses of qualified, advanced-degree U.S. students.

Although the resident staff wishes to be as helpful as possible to visitors, its responsibility is limited to giving advice and initial assistance for the efficient use of the instruments. The Observatory staff and assistants will not do observing for visitors except under emergency conditions.

In addition to the telescopes on Kitt Peak, there are at the Tucson headquarters a number of laboratory instruments, such as an electronic digital computer, a Hilger microphotometer, a Cary monochromator and spectrometer, measuring machines for direct photographs and spectrograms, a spectrocomparator, and binocular microscope viewers. The main Observatory library, electronics and photographic laboratories, and the instrument and optical shops are also located in the Tucson headquarters buildings.

Depending upon availability of office space, astronomers on sabbatical or other long-term leave may work at the Observatory while in residence in Tucson.

The Observatory staff welcomes inquiries from those astronomers and graduate students who have research programs that may merit the use of the Kitt Peak National Observatory facilities.

N. U. Mayall
Observatory Director
Kitt Peak National Observatory,
Tucson, Arizona

Resolution Adopted by American Astronomical Society, June 20, 1961, at Nantucket, Massachusetts

The Council and Members of the American Astronomical Society have studied the proposed project, West Ford, as described in a series of papers in the *Astronomical Journal* (*Astron. J.* **66**, 105–118, 1961). If the project is successfully carried out according to the published plans, it will result in a belt of orbiting dipoles around the earth which will be barely detectable by astronomers and radio astronomers with present techniques when observations are carried out from the ground. The experimental belt could, however, interfere seriously with delicate and important observations from satellite observatories scheduled to begin operation within the next two to three years, unless the lifetime of the belt is sufficiently limited. Consideration also of the rapid gains that can confidently be expected to occur in the sensitivity of astronomical measurements during the next few years makes it imperative to guard against the irreversible contamination of space. The Society is even more gravely concerned at the harm that a future operational belt or belts might cause to astronomical observations, and also calls attention to the interference that can be expected from proposed systems of passive and active communication satellites.

In the light of the foregoing considerations, the Society resolves as follows:

1. *The American Astronomical Society strongly opposes any contamination of space that is detrimental to the conduct of basic scientific research.*
2. *The Society reaffirms its previous resolution in support of world-wide frequency allocations for radio astronomy as a matter of great and increased urgency.*

ERRATA

Astron. J. **53**, 6.

For $M_0=350^{\circ}.56422$ read $M_0=353^{\circ}.56422$.

(Communicated by the author, Dr. Paul Herget.)

Astron. J. **65**, 385.

At JDE 2434980.5: for $M_0=1^{\circ}.41280$ read $1^{\circ}.84164$.

At JDE 2437420.5: for $M_0=0^{\circ}.81742$ read $2^{\circ}.32024$.

No other parts of the work are affected.

(Communicated to the author by Dr. J. G. Porter.)

Astron. J. **63**, 338.

Table 1. No. 1: for $+1^{\circ}990$ read $+0^{\circ}990$.
No. 2: for $+1^{\circ}989$ read $+0^{\circ}989$.
Delete stars Nos. 23, 26, and 28.
No. 34 for $+5^{h}41^{m}.6$ read $+5^{h}25^{m}.6$.

(The authors express their thanks to Mr. Henry Giclas of the Lowell Observatory for calling their attention to these errors.)

Astron. J. **66**, 46.

The final paragraph of the abstract by Hindman, McGee, Carter, and Kerr, reading "The peak . . . per year," has been misplaced through editorial accident. This paragraph should conclude the abstract by McGee and Murray on page 48.

NEW BOOKS RECEIVED

Mécanique Céleste, by F. Tisserand. Published by Gauthier-Villars, Paris, 1960. Vol. I, 50 N.F.; Vol. II, 60 N.

Photographically reproduced in paperback binding ($6\frac{1}{8}\times 9\frac{3}{8}$ inches) from the first two volumes which fir appeared in 1889 and 1891, respectively. According to the Preface of A. Danjon, all known typographical erro have been corrected; otherwise the volumes have not been revised.

Tisserand's *Mécanique Céleste* is deservedly famous for its lucid exposition. Even after 70 years, there is muc in these two volumes on which it would be difficult to improve.

Volumes III and IV are still available in the original edition.

Methods of Celestial Mechanics, by Dirk Brouwer and Gerald M. Clemence. Published by Academic Press Inc New York and London, 1961. Price $15.50.

Workers in the field have long felt the need for an authoritative, modern treatise which is simultaneously of u to advanced students and research workers. The present volume fills this need most successfully. Further th treatment is built up sufficiently from first principles to permit use of the book for self-study, as an introductor text for graduate instruction, or as a reference volume. The book establishes a solid balance between theoretic treatment and practical applications of the subject. Particularly helpful are worked-out numerical examples i the chapter on numerical integration of orbits.*

An Introduction to Celestial Mechanics, by T. E. Sterne, Series No. 9, Interscience Tracts on Physics and Astronom Published by Interscience Publishers, Inc., New York. Price $4.50 (cloth) and $2.50 (paper).

A competently written introduction to the basic topics of celestial mechanics, followed by applications to th problem of artificial satellite motion (including effects of atmospheric drag), and a chapter on numerical integr tion. The author has succeeded in presenting this material clearly and attractively. Yet many readers may fe the need to consult more elaborate treatises. This applies, for example, to the indication of the character of gener planetary and lunar theories (pp. 108–115), but also to some sections in the earlier chapters. This is, of cours unavoidable in such a small book and does not detract from its considerable merits.

---

* The senior Astronomical Journal editor wishes to disassociate himself from responsibility for the above notice which was kind contributed by another reviewer.